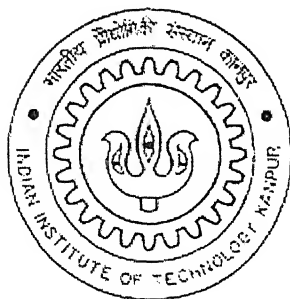


Development of modified carbon membranes for the separation of chromic acid

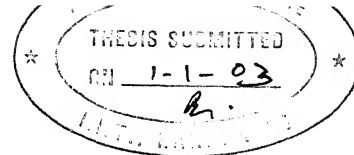
*A thesis submitted
in partial fulfillment of the requirements
for the degree of
Master of Technology*

By
Nanda Kishore



DEPARTMENT OF CHEMICAL ENGINEERING
Indian Institute of Technology, Kanpur
DECEMBER, 2002

CERTIFICATE



This is to certify that the thesis entitled **“Development of modified carbon membranes for the separation of chromic acid”** is the original work of Mr. Nanda Kishore carried out under my supervision, and has not been submitted elsewhere for the degree of Master of Technology.



(Anil Kumar)

Professor,
Department of Chemical Engineering,
Indian Institute of Technology,
Kanpur-208016,
India.

20 May 2003
पुस्तकालय
म. वि. वि. पुस्तकालय

अवधि क्र० A 143444



A143444

Dedicated to the

LORD BALAJI

Acknowledgement

It has been my dream to have the meaning of good research and I fulfilled it, under the guidance of my thesis supervisor, **Prof. Anil Kumar**. I gratefully acknowledge him for his inspiring guidance, friendly affection, unending encouragement and valuable suggestions. My association with him has been a learning experience on the different aspects of life. His positive and methodological approach continues to enlighten my path.

I would like to thank **Prof. P.K. Bhattacharya**, who's course on the membrane separation process, have given me the basic understanding about the membranes. I also sincerely thank all the faculty members of Chemical Engineering Department, IIT Kanpur. My sincere thanks to **Prof.V. Chandrashekar** and his students, for their kind help to have the TGA. I am also thankful to the staff members of the SEM and XRD sections of ACMS. I would also like to thank Mr. Sarath for providing Raman spectra and Mr. Pandey for FT-IR analysis and EA.

My special thanks to my senior lab mates Mr. G. Pugazhenthir and Mr. Anupam Shukla. I was not able to move anymore forward in this work, but their kind help made me to complete my thesis work. My lab mates Dr.G.S. Mishra, Jhansi and Anisia, need a word of appreciation for making the lab an ideal work place. I also thankful to Sharmaji, Vishwakarmaji, Virdiji, Nagendraji and Chhotu for their constant help.

I am also thankful to all of my classmates and friends, who made my stay so comfortable at IITK. My special thanks to my friends Madan, Rajesh, Pavan, Laxman, Jhansi, Anu, Hima, Sujatha, Ravi, and Shankar I also like to thank Narasi and Malli, who made me to feel homely at IITK by creating small tensions and sharing great pleasure.

Finally, I would like to thank Leela for sharing all my sorrows and pleasures even being miles away from me physically, but I feel she is always with me to making me smile as and when I wish. Indeed, I'm deeply indebted to my parents, who are the starting and ultimate goal of my life, their love and blessings continue to be my strength.

Nanda Kishore

December'2002

ABSTRACT

A new technique has been developed for forming the porous carbon-clay composite membranes. The resol polymer (300-700 mol.wt., 60% solution in ethanol) has coated on a clay support (cationic in nature), by knife coating technique. To get a non-interpenetrating polymer, the ceramic support was dipped in xylene prior to coating of the polymer and after coating it is allowed to dry before cross-linking and subsequently carbonized in a closed chamber. The composite membrane thus formed have been nitrated using NO_x (a mixture of NO and NO_2) by the gas phase reaction at 200°C for 32 hours which can further be reduced to amine groups by treating with hydrazine hydrate. The FT-IR analysis has shown a strong peak of the nitro group, which further disappeared upon the amination reaction. The Raman spectrum of the carbon membrane shows the G- and D-mode peaks, which on modification disappear. The XRD of the unmodified membrane consists of $[0\ 0\ 2]$ and $[1\ 0]$ planes of the graphite which after the modification do not show the $[1\ 0]$ plane and the resultant material becomes more amorphous. The MWCO of the membranes have been determined and is found to be 7500 and 14000 for the unmodified and nitrated membranes respectively. This suggests that by the nitration, the etching action of NO_x cause increase in pore size of the membrane. The separation experiments were carried out using 1000ppm aqueous chromic acid solution and gave 70% rejection. The water and solute flux for the modified membranes are greatly enhanced compared to those for the unmodified membrane.

Contents

List of Tables	i
List of Figures	ii

Chapter-1

1.1	Introduction	1
1.2	Literature review	4
1.3	Objective of the present work	10

Chapter-2

Experimental section	11
2.1 Preparation of macroporous clay supports	11
2.2 Synthesis of resol type phenol-formaldehyde resin	11
2.3 Membrane Casting	13
2.4 The modification of carbon membrabe by gas phase nitration of membranes using NO _x	13
2.5 Amination of nitrated carbon-clay composite membranes	14
2.6 Characterization of carbon-clay composite membranes	15
2.6.1 Elemental analysis (EA)	15
2.6.2 Thermogravimetric analysis (TGA)	15
2.6.3 Fourier Transmission Infrared Spectroscopy (FT-IR)	15
2.6.4 Scanning Electron Microscope (SEM)	16
2.6.5 Raman specroscopy	16
2.6.6 Small angle X-ray diffraction (XRD)	16
2.6.7 Molecular weight cut-off (MWCO) measurements in ultrafiltration cells	16
2.7 Experimental set up	17
2.8 Permeate flux and ultrafiltration experiments	17
2.9 Ultrafiltration experiment using aqueous chromic acid	18

Chapter-3

Results and discussions	25
3.1 Development of the clay supports	25
3.2 The Calcining process	26
3.3 The resol formation	27
3.4 The membrane casting	29
3.5 The gas phase nitration of the carbon-clay composite membranes	29
3.6 Amination of the nitrated carbon-clay composite membranes	30
3.7 Elemental analysis (EA)	30
3.8 Thermogravimetric analysis (TGA)	30
3.9 FTIR analysis	31
3.10 Structural analysis of the membranes by scanning electron microscope (SEM)	32
3.11 Raman spectroscopy	32
3.12 Small angle X-ray diffraction (XRD)	33
3.13 Determination of Molecular weight cut-off of the membranes	33
3.13 Separation experiment using aqueous solution of chromic acid	34

Chapter-4

Conclusions	55
References	56

List of Tables

Table 1.1	Some of the industrial important membrane processes and their applications	2
Table 1.2	some of the carbon membranes prepared from different precursor materials	6
Table 2.1	Chemical formulae and density of clay materials	19
Table 3.1	Elemental analysis of resol at different heat treatment temperatures	36
Table 3.2	The R values for the unmodified, nitrated and aminated membranes	36
Table 3.3	Calibration data for different molecular weight of PEG solutions	36
Table 3.4	Molecular weight cut-off of the unmodified carbon-clay composite membrane	37
Table 3.5	Molecular weight cut-off of the nitrated carbon-clay composite membrane	38
Table 3.6	Calibration data for chromic acid solution of different concentrations	38
Table 3.7	Results of the separation experiments done with the unmodified carbon-clay composite membrane with 1000 mg/l aqueous chromic acid solution	39
Table 3.8	Results of the separation experiments done with the nitrated carbon-clay composite membrane with 1000 mg/l aqueous chromic acid solution	40
Table 3.9	Results of the separation experiments done with the nitrated carbon-clay composite membrane with 1000 mg/l aqueous chromic acid solution	41

List of figures

Figure 2.1: The membrane casting set up	21
Figure 2.2: The closed chamber for carbonization	
(A) Top view of the chamber, (B) The side view of the lid	22
Figure 2.3: The nitration reactor filled with NO _x	23
Figure 2.4: The ultrafiltration experimental set up	24
Figure 3.1: Thermogravimetric analysis of the cured resin under N ₂ atmosphere	42
Figure 3.2: The FT-IR spectrum of the resol type PF resin catalyzed by NaOH	43
Figure 3.3: The FTIR spectra of the (A)Unmodified, (B)Nitrated and (C)Aminated Carbon membranes	44
Figure 3.4: The SEM photograph of the top surface of the clay support	45
Figure 3.5: The SEM photograph of the top surface of the unmodified carbon membrane	45
Figure 3.6: The SEM photograph of the topsurface of the nitrated carbon membrane	46
Figure 3.7: The SEM photograph of the cross section of the carbon membrane	46
Figure 3.8: The raman spectra of the (A) Unmodified, (B) Nitrated and (C) Aminated carbon membranes	47
Figure 3.9 The XRD patterns of the (A) Unmodified, (B) Nitrated and (C) Aminated carbon membranes	48
Figure 3.10: Calibration curve for Polyethylene Glycol	49
Figure 3.11: The Molecular Weight Cut-Off curves for the unmodified and nitrated carbon membranes	50
Figure 3.12: Calibration curve for chromic acid solution of varying concentrations	51
Figure 3.13: Pure water flux curves for the unmodified, nitrated and aminated carbon membranes	52
Figure 3.14: Solute flux curves for the unmodified, nitrated and aminated carbon membranes	53
Figure 3.15: The Rejection curves for the unmodified, nitrated and aminated carbon membranes	54

CHAPTER-1

1.1 Introduction:

Membranes are barriers in which separation of two or more distinct species occur in presence of one or combination of the driving forces. The latter could be pressure gradient, concentration gradient, electrical potential gradient, partial pressure etc. the barriers are mostly solids (polymeric or in-organic membranes) or liquids (liquid membranes). Some of the properties of the barrier effecting the separation are:

- a. Their chemical nature (organic or in-organic)
- b. Nature of openings (homogeneous or microporous)
- c. Presence of charges and
- d. Degree of asymmetry

In symmetric membranes pore size across the thickness is the same. Since the flux across any barrier is inversely proportional to its thickness, attempts have been made to develop asymmetric membrane, in which the separating (skin) layer is very thin in the order of 10^{-6} to 10^{-9} m and is supported by a non-separating, relatively thick micro (or macro) porous support.

The membrane separation process chosen depends upon the nature of driving force, nature of mixture to be separated, type of membrane used and its applications (as given in table 1.1). The pressure driven process is classified as Reverse Osmosis (RO), Microfiltration (MF), Ultrafiltration (UF) and Nanofiltration (NF). Electrically mediated separations are classified as Electrodialysis and Electro Osmosis. In RO, the solvent is adsorbed on the higher-pressure side of the membrane, dissolves in to the membrane due to its osmotic pressure and is desorbed from the lower-pressure side of the membrane. Desalination is the main application of the RO and the operating pressure range is 25-135 atm. In UF, separations of higher molecular weight materials greater than 500 from aqueous and organic streams occur by the size exclusion through the microporous membranes. UF is an energy effective process since its operating pressure range is smaller (0.5-10 atm). In NF, the mechanisms of separation are sieving as well as electrostatic interactions between membrane surface and permeating solutes. The operating pressure of the NF lies between that needed for RO and UF.

Table1.1: Some of the industrial important membrane processes and their applications¹:

S. No	Membrane separation process	Membrane type	Driving force	Applications
1	Microfiltration	Symmetric microporous	Hydrostatic pressure	Clarification, sterile filtration
2	Ultrafiltration	Asymmetric microporous	Hydrostatic pressure	Separation of macromolecular solution
3	Nanofiltration	Asymmetric microporous	Hydrostatic pressure	Separation of small organic compounds and selected salts from solutions
4	Hyperfiltration (Reverse Osmosis)	Asymmetric, composite with homogeneous skin	Hydrostatic pressure	Separation of microsolutes and salts from solutions
5	Gas permeation	Asymmetric or composite homogeneous or porous polymer	Hydrostatic pressure, concentration gradient	Separation of gas mixtures

S. No	Membrane separation process	Membrane type	Driving force	Applications
6	Dialysis	Symmetric microporous	Concentration gradient	Separation of microsolutes and salts from macromolecular solutions
7	Pervaporation	Asymmetric, composite	Concentration gradient, vapour pressure	Separation of mixtures of volatile liquids
8	Vapour permeation	Composite	Concentration gradient	Separation of volatile vapour and gases
9	Membrane distillation	Microporous	Temperature	Separation of water from non-volatile solutes
10	Electrodialysis	Ion-exchange, homogeneous or microporous polymer	Electrical potential	Separation of ions from water and non-ionic solutes
11	Electro-osmosis	Microporous charged membrane	Electrical potential	Dewatering of solutions of suspended solids

S. No	Membrane separation process	Membrane type	Driving force	Applications
12	Electrophoresis	Microfiltration membranes	Electrical potential, hydrostatic pressure	Separation of water and ions from colloidal solutions
13	Liquid membranes	Microporous, liquid carrier	Concentration reaction	Separation of ions and solutes from aqueous solutions

1.2 Literature review:

Hsich² has provide a review on inorganic membranes classifying it into porous and non-porous (dense) membranes. Some metals like palladium, silver and their alloys, solid electrolytes like zirconia and nickel metal falls under non-porous inorganic membranes. Porous inorganic membranes could be alumina, titania, zirconia, carbon, silica, zeolites etc. In addition porous inorganic membranes could have asymmetric or symmetric porous in nature with pores of about 0.3nm size, which usually work as sieves for large molecules or particles. Among these, in the present context, the microporous inorganic membranes prepared from precipitated oxides (silica-based membranes), zeolites and carbon are of considerable importance. The carbon membranes are usually prepared by carbonization of polymeric films in an inert atmosphere, which leads to the formation of a thin carbon layer with pores smaller than 1nm. Different authors have reported (see table1.2) that the controlled carbonization of polymers like polyimide, poly (furfuryl alcohol) and poly (vinylidenechloride) which give rise to crack-free carbon molecular sieve films³. In practice, carbon membranes have been prepared in two main configurations: (a). Unsupported carbon membranes (flat, capillary tubes, or hollow fiber) and (b). Supported carbon membranes (flat or tubular).

Some of the advantages of carbon membranes are given below:

1. Carbon membranes are mechanically much stronger and can withstand higher-pressure differences⁴.
2. Carbon membranes have higher elastic modules and lower breaking elongation than the polymeric membrane⁵.
3. Carbon membranes do not possess compaction and swelling problem².
4. Carbon membranes offer the advantage of operation in environments prohibitive to polymeric materials and have superior stability in the presence of organic vapor or solvent and non-oxidizing acids or bases environments⁶.
5. Carbon membranes are ideal for corrosive applications.
6. Carbon membranes are far more stable thermally than polymeric membrane⁷.
7. Carbon membranes have the ability to be back flushed, steam sterilized or autoclaved².
8. Carbon membrane is very brittle and fragile. Therefore, it requires more careful handling⁴.
9. Carbon membranes require a pre-purifier for removing traces of strongly adsorbing vapors, which can clog up the pores⁴.

Table 1.2: Some of the carbon membranes prepared from different precursor materials:

S. No.	Precursor Material	Coating technique	Configuration	Carb ⁿ temp (°C)	Separating system	Reference
1	Polyamic acid	Spin coating	Flat	550	O ₂ /N ₂ CO ₂ /CH ₄ He/N ₂ CO ₂ /N ₂	8
2	PF resin (Novolac type)	Spin coating	Flat	500 to 1000	CO ₂ /CH ₄	9
3	PF resin (Novolac type)	Dip coating	Tubular	700	O ₂ /N ₂ CO ₂ /N ₂ CO ₂ /CH ₄	10
4	Poly (furfuryl alcohol)	Spray coating	Flat	600	O ₂ /N ₂	11
5	Poly (furfuryl alcohol)	Spray coating	Flat	500	O ₂ /N ₂	12
6	PF resin (Resole type)	Spin coating	tubular	800	CO ₂ , He permeation	13

S. No.	Precursor Material	Coating technique	Configuration	Carb ⁿ temp (°C)	Separating system	Reference
7	Acid washed Coconut Charcoal	—	Flat	—	Vegetable & Fruit extracts	14
8	PF resin (Novolac type)	Dip coating	Tubular	700	O ₂ /N ₂ CO ₂ /N ₂ He/N ₂ CO ₂ /CH ₄	15
9	Poly (furfuryl alcohol)/ Poly ethylene Glycol	Spray coating	Flat	600	Water Flux & Dextran Separation	16
10	Methane	Chemical vapor deposition	Tubular	1000	N ₂ flux	17
11	Poly (furfuryl alcohol)	Dip coating	Tubular	650 to 900	—	18
12	Poly etherimide	Dip coating	Tubular	500	CO ₂ /CH ₄	19

S. No.	Precursor Material	Coating technique	Configuration	Carb ⁿ temp (°C)	Separating system	Reference
13	Poly (furfuryl alcohol)	Brush coating	Flat	600	O ₂ /N ₂ H ₂ /N ₂	20
14	PF resin (Novolac Type)	Dip coating	Tubular	900	O ₂ /N ₂ H ₂ /N ₂ H ₂ /CH ₄ H ₂ /CO ₂ CO ₂ /N ₂ CO ₂ /CH ₄	21
15	Polyimide	—	Hollow fiber	500 and 550	O ₂ /N ₂	22
16	PF resin (Novolac type)	Dip coating	Tubular	700	O ₂ /N ₂ He/N ₂ CO ₂ /N ₂ CO ₂ /CH ₄	23
17	Poly (furfuryl alcohol)	—	Flat	500	CH ₄ /C ₂ H ₆	24
18	PF resin (Novolac type)	Dip coating	Tubular	700	O ₂ /N ₂ CO ₂ /N ₂ CO ₂ /CH ₄	25

S. No.	Precursor Material	Coating technique	Configuration	Carb ⁿ temp (°C)	Separating system	Reference
19	PF resin	—	Flat	800 to 950	H ₂ /N ₂ O ₂ /N ₂	26
20	Polyimide	—	Hollow fiber	550 to 800	H ₂ /N ₂ O ₂ /N ₂	27
21	Poly (amic acid)	Dip coating	Tubular	700	C ₂ H ₄ / C ₂ H ₆ and C ₃ H ₆ / C ₃ H ₈	28
22	Poly (vinylidene chloride)	—	Flat	1000	H ₂ /CH ₄ H ₂ /C ₂ H ₆ H ₂ /C ₃ H ₈ H ₂ /C ₄ H ₁₀	29
23	Poly (furfuryl alcohol)	—	Tubular	800	—	30

1.3 Objective of the present work:

Since, the increasing contaminant level of metal salts in water especially those of chromium, mercury, cadmium are found to occur as industrial waste. These are non-biodegradable and have a carcinogenic effect³¹. The conventional process of precipitation is expensive due to additional chemicals required for treatment and sophisticated mechanical equipment for separation is needed for this purpose. Literature reports³¹⁻⁴⁰ that the chromium wastes can be recovered from water solution using membrane separation techniques. Membranes having molecular weight cut-off (MWCO) less than 5000 have been reported in patent literature and in view of this we have decided to prepare membranes having MWCO less than 5000. Since carbon membranes have many advantages as mentioned earlier, we decided to prepare porous carbon membrane, which can serve, for this purpose.

In this work, we have first coated a clay support with resol type phenol-formaldehyde (PF) resin followed by carbonization to obtain porous carbon membranes. The modification of the porous carbon membrane is carried out with NO_x gas (a mixture of NO and NO_2) and the nitro group on the carbon surface can further be reduced to amine ($-\text{NH}_2$) group by reaction with hydrazine hydrate. The advantage with amine modification is that the hydrophilicity of the membrane is improved. The performance of the porous carbon membrane and the modified porous carbon membranes studied by separating the chromic acid solution.

Chapter-2

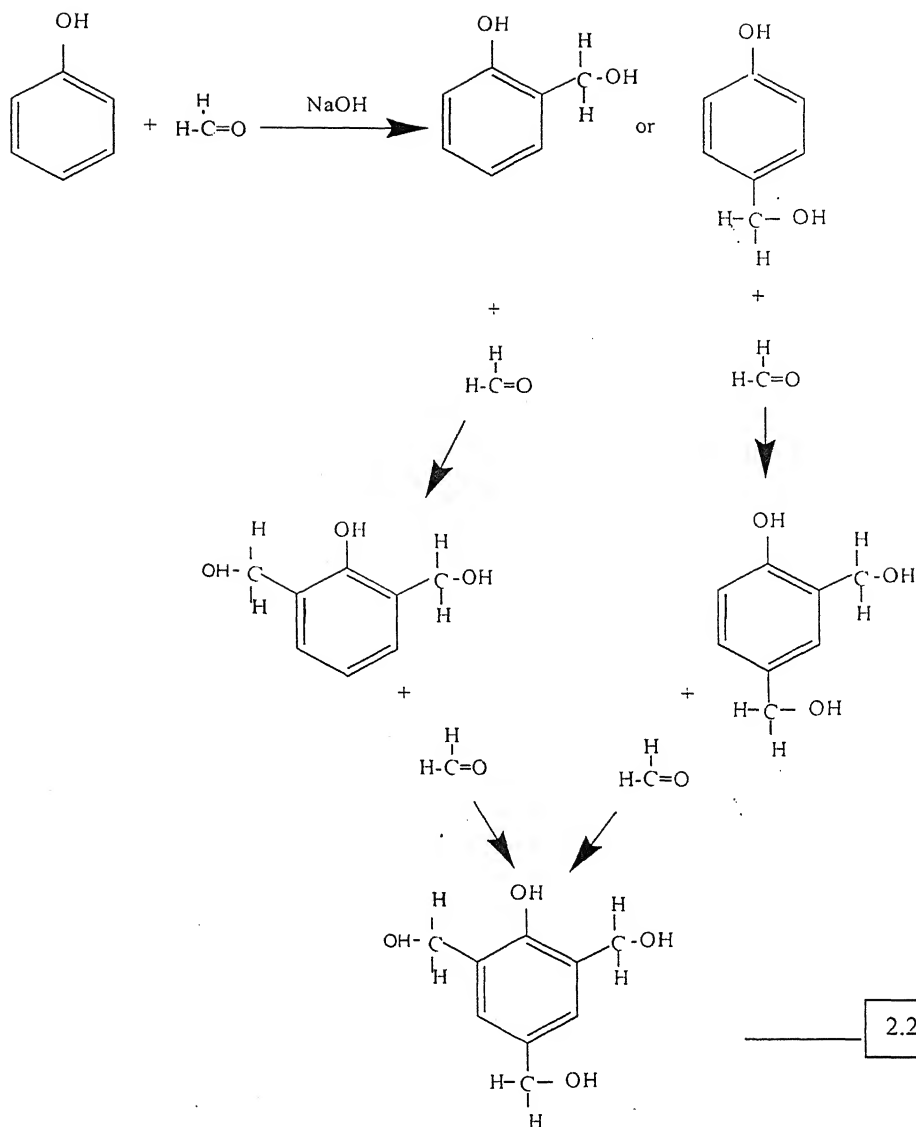
Experimental Section

2.1 Preparation of macroporous clay support:

The macroporous clay supports have been prepared from the clay mixture with the composition given in table 3. These clay powders were first thoroughly mixed in a vessel and made as a paste with 65 ml of distilled water. On the gypsum surface this paste spread in the form of flat, circular discs. The required size was cut using a stainless steel ring of 76mm internal diameter and 5mm thickness. The stainless steel ring is later removed carefully to avoid cracking of the wet discs. This was then allowed to dry (for 24 hours) after covering with a firebrick, to ensure the slow water removal. Further stages of drying are carried out at 100⁰C for 12 hours, then at 250⁰C for 24 hours to get the 'green' disc. Then these supports are fixed in vertical position on a firebrick and calcined at 900⁰C for 6-8 hours. By this process, these supports become very hard, rigid and macroporous in nature. The calcined supports are slowly cooled down to room temperature and polished using a silicon carbide (No. C-220) in order to get flat, circular and smooth support. This final support is of 2-3mm thickness and 66mm diameter.

2.2 Synthesis of resol-type phenol-formaldehyde resin:

The phenolic resins are condensation products of phenol and formaldehyde. The low molecular weight (300-700 mol.wt.)⁵⁵resol-type PF resin is formed in presence of basic catalyst (sodium hydroxide) and as the reaction continues, methylol phenols condense to form methylene bridges. The reaction forming the substituted phenol is given below:



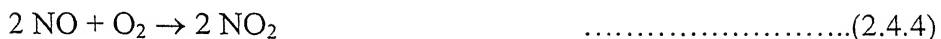
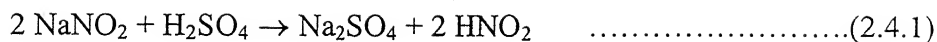
The resol preparation had been carried out in a 1000ml three necked glass reactor equipped with reflux condenser, stirrer and thermometer. To the reaction vessel, a mixture of 94g(1mole) of phenol, 123g (1.5mole) of 37% aqueous formaldehyde and 5g of sodium hydroxide added^{42, 43}. The reaction mixture is slowly heated and maintained at 95°C with proper stirring. The condensation to form resols occurs in one hour, but the reaction is continued for 5 hours at same temperature to obtain an extremely viscous reaction mass. The product is taken out of the reaction vessel and used for the membrane casting.

2.3 Membrane casting:

Before coating the PF resin on smoothly polished, macroporous, flat and circular clay support, the support is dipped in xylene, which is a non-solvent for resol polymer. On dipping the support, xylene displaces the air present inside its pores and then it is placed over polyurethane foam, which soaked in xylene as shown in figure 2.1. This ensures that the polymer does not go into the pores of the support and after approximately 60-75 minutes, it is coated with a 60% of resol in ethyl alcohol using a knife. The coated support is allowed to dry in air for one hour and after this, it is cured for 2 hours at 60°C , followed by 12 hour at 120°C in an oven. After that, the clay-resol composite is carbonized in a closed chamber (see figure 2.2) at 500°C with the heating rate of $2.5\text{-}3^{\circ}\text{C}$ and maintained at the final temperature for half an hour. After cooling to the room temperature the final clay-carbon composite membrane obtained, which is porous in nature. Before it is used for separation experiment, it is flushed with water at high pressures, so as to remove the strongly adsorbed gases present in side the pores of membrane. With the knowledge of the weight of the polymer, density of the polymer and area of spreading, one can calculate the membrane thickness and is of the order of $10\text{-}20\mu\text{m}$.

2.4 The modification of carbon membrane by gas phase nitration using NO_x :

The gas phase nitration of the carbon membrane is done in a three-liter volume reactor as shown in figure 2.3. The reactor is made of glass and equipped with a stainless steel lid. The lid has a brass cap having an opening of 1-2mm diameter, which is sealed with silicon-rubber septum. A double necked flask is used to produce NO_x by reacting sodium nitrite (NaNO_2 , 10gmole) with sulfuric acid (98% H_2SO_4 , specific gravity = 1.98, 25ml) and ferrous sulphate (FeSO_4 , 1gmole). One neck of the flask is closed with rubber septum for withdrawing the gas with a 50ml syringe. The production of NO_x is according to the following mechanism:



The carbon membrane is kept inside the reactor. A vacuum is created inside the reactor by vacuum pump. The valve should be closed such that at the reaction temperature, when the NO_x is introduced inside the reactor, the total pressure should not exceed the atmospheric pressure to avoid leakage. Approximately 500ml of NO_x is introduced into the reactor for each run. The nitration reaction is carried out at 200°C for 32 hours. The increase in weight due to nitration is noted down. The membrane has now nitro- groups, confirmed through FT-IR spectra.

2.5 Amination of nitrated porous carbon membranes:

Amination of the nitrated porous carbon membrane is carried out with hydrazine hydrate. The nitrated membrane is placed at the bottom of a beaker and about 100ml of 60% hydrazine hydrate is poured over it and the beaker is made airtight by covering the mouth with aluminium foil. The membrane is refluxed for 12hours at 75°C in a silicon oil bath. After the reaction, the membrane is washed thoroughly with distilled water and dried in an oven at 60°C . The membrane has now amine groups attached to the surface, which is confirmed through FT-IR spectra.

2.6 characterization of carbon-clay composite membranes:

The carbon composite membranes are characterized using the following features:

1. Elemental analysis (CHN Analysis)
2. Thermogravimetric analysis (TGA)
3. Fourier transmission infrared spectroscopy (FT-IR)
4. Scanning electron microscopy (SEM)
5. Raman spectroscopy
6. Small angle X - ray diffraction (XRD)
7. Molecular weight cut-off (MWCO) measurements in ultrafiltration cells

2.6.1 Elemental analysis:

The weight percentage of the elements C, H, N, O is determined by using EA1110-CHNS-O Analyzer provided by Thermoquest CE instruments. The membrane is first ground into a fine powder, washed with distilled water and dried at 60°C before the analysis. All the samples prepared for the analysis are dry and ash-free.

2.6.2 Thermogravimetric analysis (TGA):

Thermogravimetric analysis of cured (at 120°C) resol was performed with Perkin Elmer Instruments, model PCB-TGA6 unit, under nitrogen atmosphere at the heating rate of 10°C/min over the temperature range from 50°C to 800°C.

2.6.3 Fourier transmission infrared spectroscopy (FT-IR):

Using Bruker, Vector 22-type FT-IR spectrometer, the functional groups present in unmodified and modified carbon membranes has been identified. Before analysis the unmodified carbon membrane first, is ground into fine powder then nitrated and aminated in similar way and at same conditions as carbon composite membranes have been modified. The modified carbon powder is 2-3 times washed with distilled water and dried in an oven at 60°C. All the FT-IR spectra are taken in KBr solution.

2.6.4 Scanning electron microscopy (SEM):

The structural morphology of the surface and the cross section of the unmodified and modified carbon composite membranes have been analyzed using Joel-Jsm (model 840A) scanning electron microscope (SEM). All membrane samples are first dipped in liquid nitrogen and then are coated with gold before carrying out the SEM analysis.

2.6.5 Raman spectroscopy:

Raman scattering of carbon is a technique for measuring the degree of sp^3 to sp^2 binding. Carbon powder obtained by crushing a block carbonized resol at same temperature as the membranes have been prepared and modified by nitration and amination reactions and analyzed for the Raman spectra in Perx 1877E triple beam spectrophotometer with $\lambda_{ex} = 514.5\text{nm}$ and $P = 100\text{mW}$.

2.6.6 Small angle X-ray diffraction (XRD):

The samples for XRD are prepared in similar way as they have been prepared for Raman spectroscopy. The XRD analysis was carried out with ISO-Debye flex 2002 X-ray powder diffractometer. The $\text{Cu } k_\alpha$ radiation was used for XRD patterns with accelerating voltage of 30kV and tube current of 20mA.

2.6.7 Molecular weight cut-off (MWCO) measurements in ultrafiltration cells:

In general, MWCO is defined as the smallest molecular weight solute, which are retained 90% by the membrane⁴⁴. We have determined the MWCO of the unmodified and nitrated carbon composite membranes by using 1wt-% aqueous polyethylene glycol (PEG) solutions of different molecular weights. The concentration of PEG is measured by refractive index (RI) using Innco refractometer. Various molecular weights of PEG used are 400, 600, 4000, 6000, 12000, 20000 and 35000. All the membranes are flushed with distilled water at 110psig before use so that to remove strongly adsorbed gases inside the pores. For measuring MWCO the applied pressure is fixed at 60psig and

permeate is collected after 24hours. PEG concentration in the feed, permeate and retentate are measured.

2.7 Experimental setup :

The detailed experimental setup is shown in figure 2.4. The set up consists of two parts, the cylindrical top part and a base plate. The entire setup is made of SS316 with a height of 240-mm and an outer diameter of 76-mm. This cylindrical cell has a volume of 1000 ml. The base plate has circular groove of 4-mm depth, which houses the membrane. The carbon composite membrane is placed inside a perforated stainless steel casing of 60-mm inner diameter and has a 2-3mm deep groove. The composite membrane is carefully filed so that it fits exactly inside the casing. The clearance between the membrane and the casing is sealed with a fast-setting epoxy resin, which is allowed to set overnight, so that it becomes a hard and water proof mass. The casing with the membrane is now placed inside the cylindrical groove of the base plate. The cylindrical cell is placed on top of the casing with an O-ring between them. The O-ring thus transfers the pressure exerted by the top cell to the casing, which prevents the membrane from getting cracked. The top cell is fixed to the base plate by nut and bolt thus making the entire set a leak proof. A high-pressure nitrogen cylinder (150 bar) which is connected to the cell by a high pressure Freon charging line (burst pressure 1500 psig) pressurizes the cell.

2.8 Permeate flux and ultrafiltration experiments:

Darcy's law³¹ for flow through porous media can describe the water flux through an ultrafiltration membrane. It states that volumetric flux is directly proportional to the applied pressure gradient.

$$J_w = K \Delta P_{applied} \dots\dots\dots 2.8.1$$

Where
$$K = \frac{1}{R_m \mu_w}$$

Where R_m = Intrinsic hydraulic resistance

J_w = Water flux

μ_w = Viscosity of water

In ultrafiltration, the rejection factor is defined as one minus the ratio of concentrations of a component 'i' on the downstream side and the upstream side of the membrane. The upstream concentration can be either in the bulk (Apparent rejection factor R_{app}) or at the membrane surface (Intrinsic rejection factor R_{int})⁴⁴. Since it is difficult to measure the solute concentration at the membrane surface we measure only the apparent rejection factor.

$$R_{app}(\%) = \left(1 - \frac{C_p^{sol}}{C_R^{sol}}\right) \times 100 \quad \dots\dots\dots 2.8.2$$

Where C_p^{sol} = Solute concentration in permeate.

C_R^{sol} = Solute concentration in retentate (in bulk).

$$R_{int}(\%) = \left(1 - \frac{C_p^{sol}}{C_m^{sol}}\right) \times 100 \quad \dots\dots\dots 2.8.3$$

Where C_p^{sol} = Solute concentration in permeate.

C_m^{sol} = Solute concentration at the membrane interface.

2.9 Separation experiments using aqueous chromic acid:

The experimental setup is as described in section 2.7. All the membranes are flushed with distilled water beforehand at 100 psig for 24 hours. This is done to remove the strongly adsorbed gases inside the pores of the membrane. For each run the cell is filled with 500 ml of 1000 mg/lit of chromic acid solution with a pH of 1. The chromic acid concentration in feed, permeate and retentate are measured using the conductivity cell in the μP based Water Analysis Kit (Model CMK 731) supplied by Century

Instruments (P) Ltd. The conductivity cell is standardized by using N/10 KCl solution. For all the experiments the cell constant is fixed at 1.04. This instrument also takes into account, the temperature dependency of the conductivity and has a resolution of 0.1 μmho . Since we are using a batch cell the concept of steady state doesn't holds good. To have consistency in experiments, the permeate is collected after 24 hours for all the runs.

Table 2.1 Chemical formulae and density of clay materials:

Sl. No.	Clay raw material	Chemical formula	Composition (wt.%)
1.	<i>kaolin</i>	$\text{Al}_2(\text{Si}_2\text{O}_5)(\text{OH})_4$	13.28
2.	Ball clay	$3\text{SiO}_2.\text{Al}_2\text{O}_3$	16.15
3.	Feldspar	$(\text{Na}, \text{Ca})(\text{AlSi}_3\text{O}_8)$	5.15
4.	Quartz	SiO_2	24.44
5.	Pyrophyllite	$\text{Al}_2(\text{Si}_2\text{O}_5)_2(\text{OH})_2$	13.54
6.	Calcium carbonate	CaCO_3	27.44

Steps for the preparation of clay supports:

- Casting on to gypsum surface or firebrick. Gypsum surface gives more consistent results.
- Clay supports dried in ambient air for 24 hours.
- Clay supports dried at 100°C for 12 hours.
- Further drying at 250°C for 24 hours.
- Calcining at 900°C for 6-8 hours.
- Surface polishing.

Specification of the final membrane:

- Effective diameter of the membrane 5.75 cm.
- Effective filtration area 26.00cm^2 .
- Support thickness 2-3 mm.
- Membrane thickness (cured resol film) $40\text{ }\mu\text{m}$ (approximately)
- Membrane thickness (after carbonization) $< 20\text{ }\mu\text{m}$ (approximately)

Specifications of the Aluminium casing:

- OD of the casing 76 mm.
- ID of the casing 68 mm.
- Height of the casing 5 mm.

Calculation of thickness from the weight of polymer:

Weight of polymer spread over the support after final drying = 0.4001g

Area of spreading = 34.212 cm^2

Density of the polymer = 2.9 g/cc

$$t \cdot \frac{\pi D^2}{4} = m/\rho$$

$$34.212 \times t = 0.1379$$

$$\text{Thickness (t)} = 40.3266\text{ }\mu\text{m}$$

\therefore The thickness of the resol film (t) = $40\text{ }\mu\text{m}$ (approximately)

\therefore The thickness of the carbon membrane (after carbonization) = $< 20\text{ }\mu\text{m}$ (approximately)

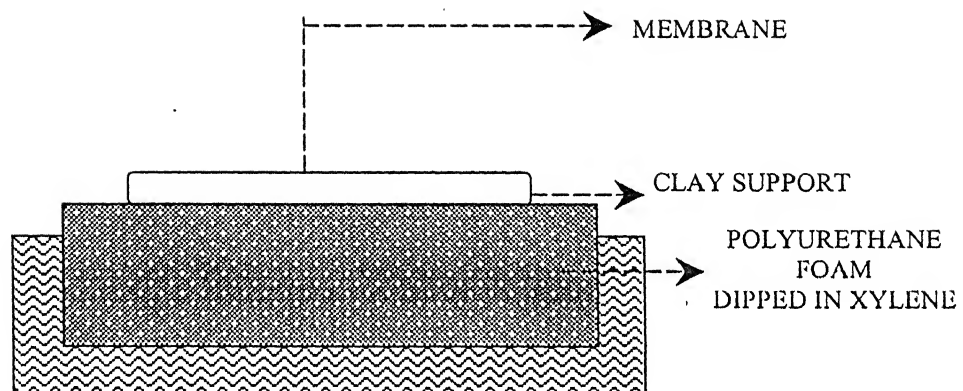
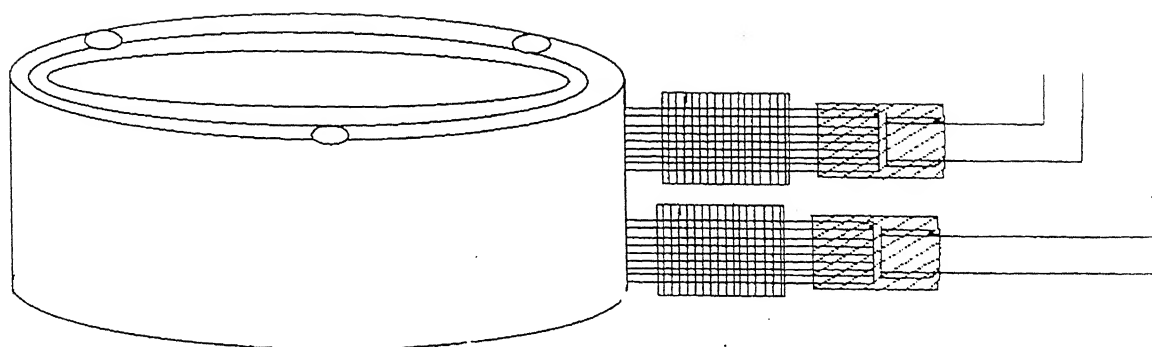


Figure 2.1 The membrane casting set up

A



B

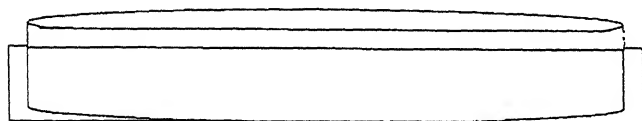


Figure 2.2 The closed chamber for carbonization (A) Top view of the chamber (B) The side view of the lid

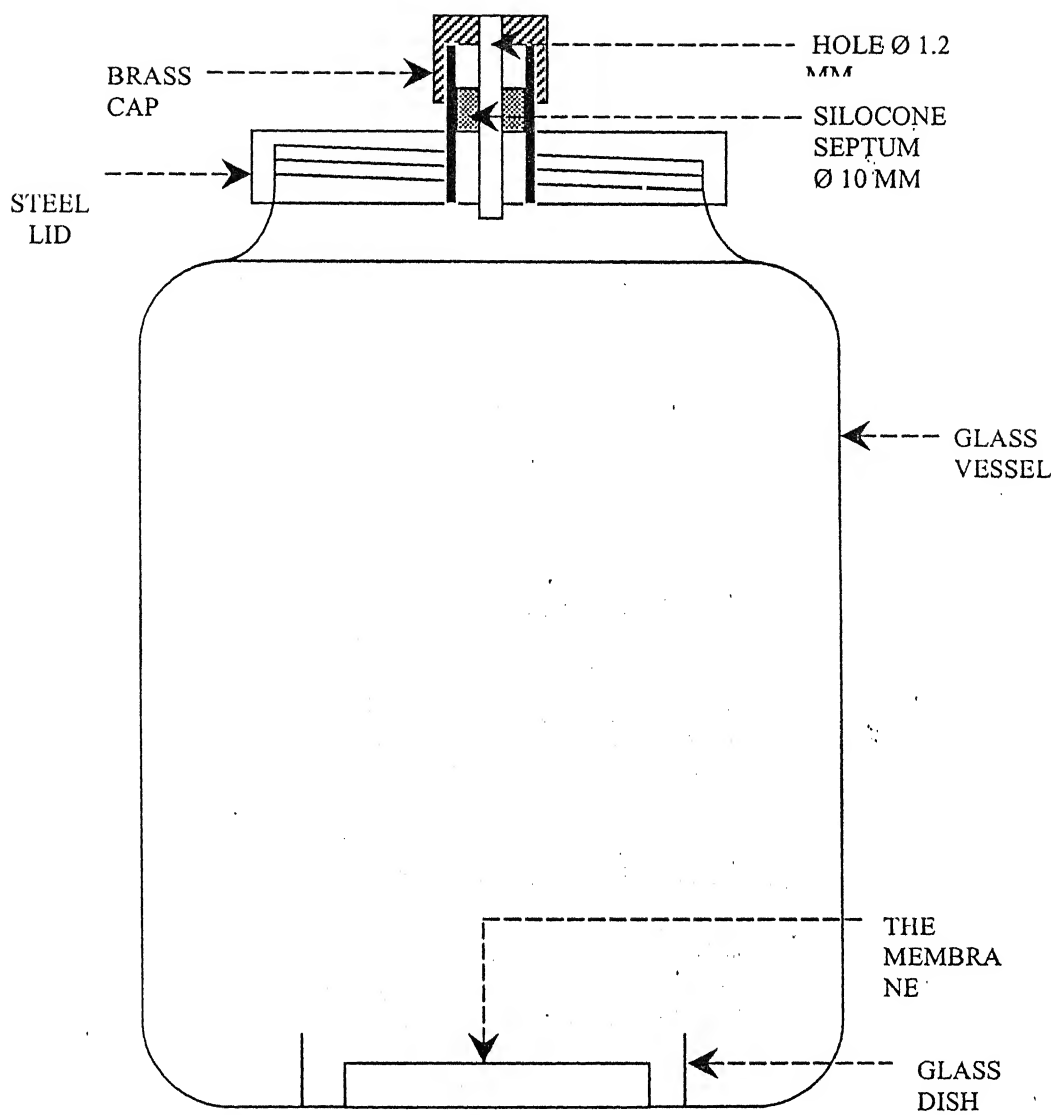


Figure 2.3: The nitration reactor

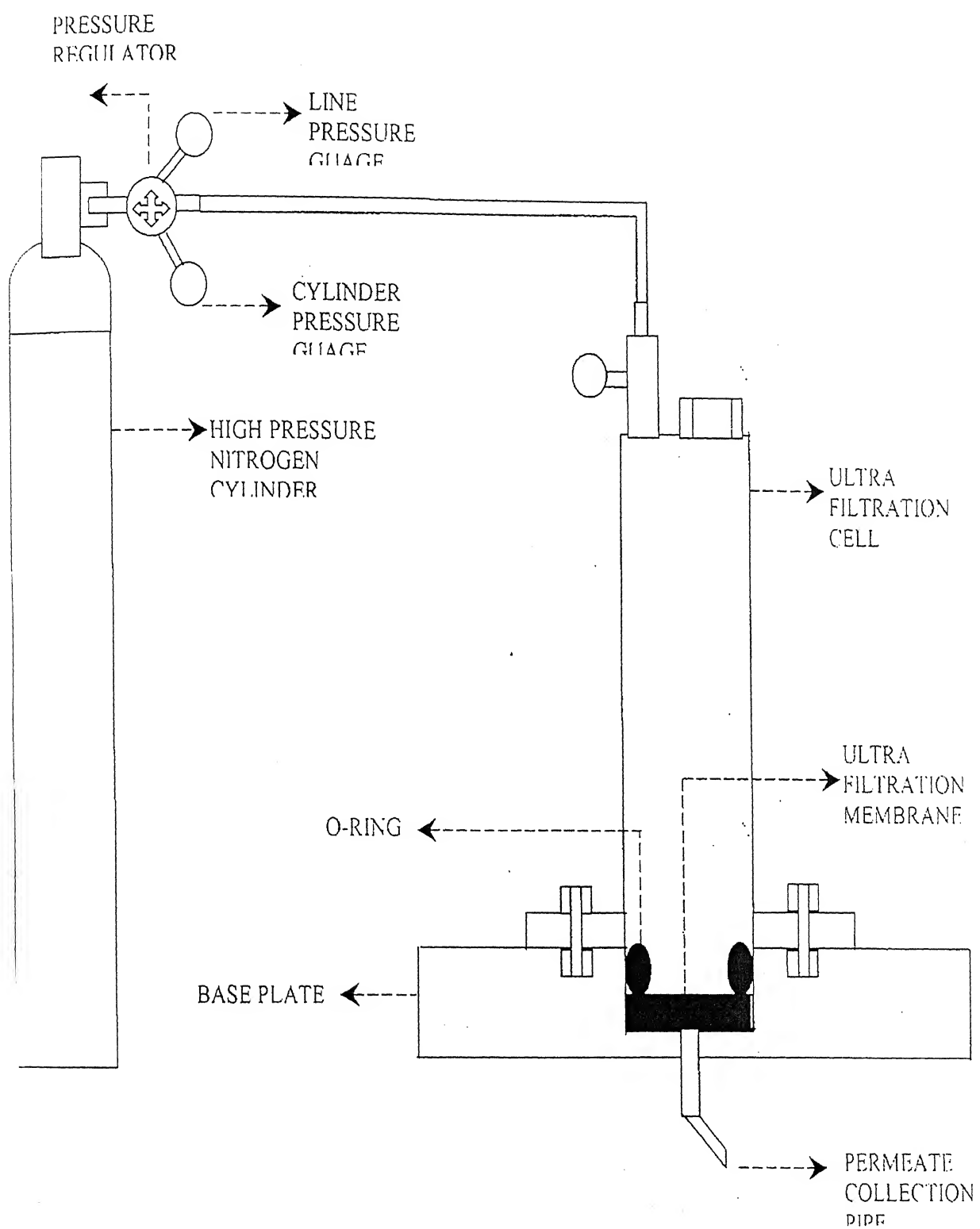


Figure 2.4 The ultrafiltration experimental set-up

Chapter-3

Results and Discussions

3.1 Development of clay supports:

For the synthesis of clay supports, various clay materials are mixed with distilled water, in the composition given as in Table 2.1 and made into a thick paste. The recipe used is a slight modification of the one given in reference (41) and as a result of this change, the clay supports are cationic in nature. This paste is molded in the form of a circular disc by using shallow stainless steel casting, which is placed over a dry and flat gypsum surface. The drying of the clay supports are carried out in 3 stages as follows:

- (a) Air drying under ambient conditions for 24 hours.
- (b) Oven drying at 100°C for 12 hours.
- (c) Oven drying at 250°C for 24 hours.

Slow drying of the clay supports is of prime importance. Non – uniform or fast or differential drying leads to the development of surface cracks. The gypsum surface also plays an important role during the drying. The supports that are molded over glass, firebrick or stainless steel surface has developed significant cracks. Surface cracks develop because of the following reasons⁴⁵:

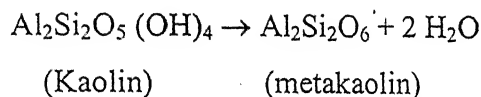
- (a) Case hardening occurs when shrinkage of surface material has ended, but the internal materials with higher liquid content continue to shrink. This lead to the development of internal tensile stress that may produce internal cracks.
- (b) Differential shrinkage leads to warping because of non-uniform drying across the thickness.
- (c) Cracks develop when surface material becomes brittle.
- (d) Mechanical resistant of shrinkage.
- (e) Contact friction between firebrick surface and the clay supports lead to surface cracks, which is characteristics feature if the product is heavy and the support is highly rough.

We have eliminated the surface cracks by the orientation of the supports in stage (b) and (c) of drying. During oven drying, the clay supports in “green” state are kept vertically in the grooves cut in firebrick. The firebrick surface, being highly water absorbing, is likely to give a faster driving force for drying than the less porous gypsum surface and hence giving rise to surface cracks.

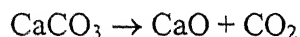
3.2 The calcining process:

After drying in stage 3, the clay supports are calcined in a furnace at 900°C for 6 to 8 hours. It is done to provide the desired mechanical strength to it. The structural changes and reactions that occur during this reaction are given below:

- (a) The clay particles condense together into a crystalline hard and rigid compact.
- (b) Water of kaolin is eliminated between 450°C and 700°C by the reaction producing metakaolin $\text{Al}_2\text{Si}_2\text{O}_6$.



- (c) Dehydration of aluminum hydrates occurs between 320 - 560°C.
- (d) The organic matter in ball clay is oxidized between 200 - 700°C.
- (e) Decomposition of calcium carbonate occurs between 200 - 700°C.



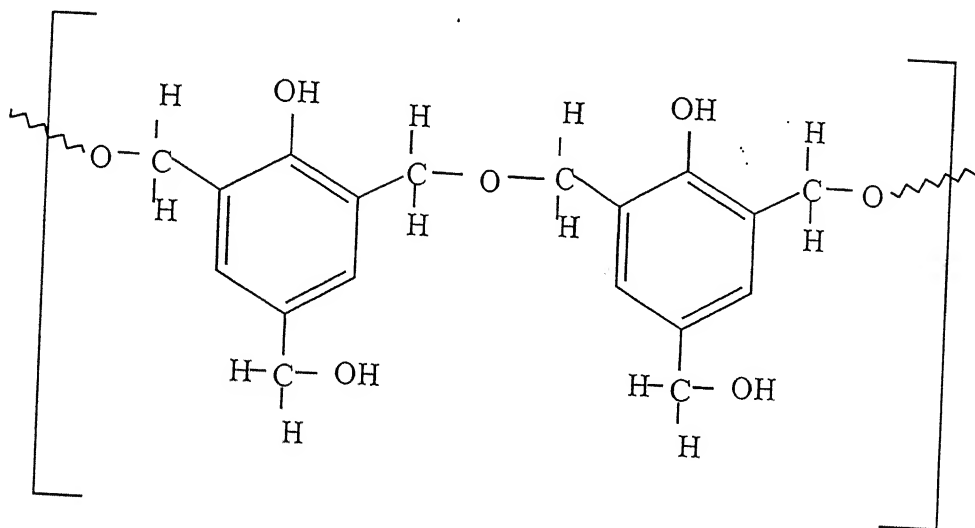
These gaseous products are expelled during calcination process and produces volume expansion and the formation of pores within the clay supports. In order to get a good, flat and porous support, the following precautions must be followed:

- (a) Complete removal of moisture from the supports prior to calcining process.
- (b) By controlled rate of heating in the furnace, thus allowing the gradual removal of gaseous products from the supports.
- (c) By vertical orientation of the clay supports during oven drying and calcining.

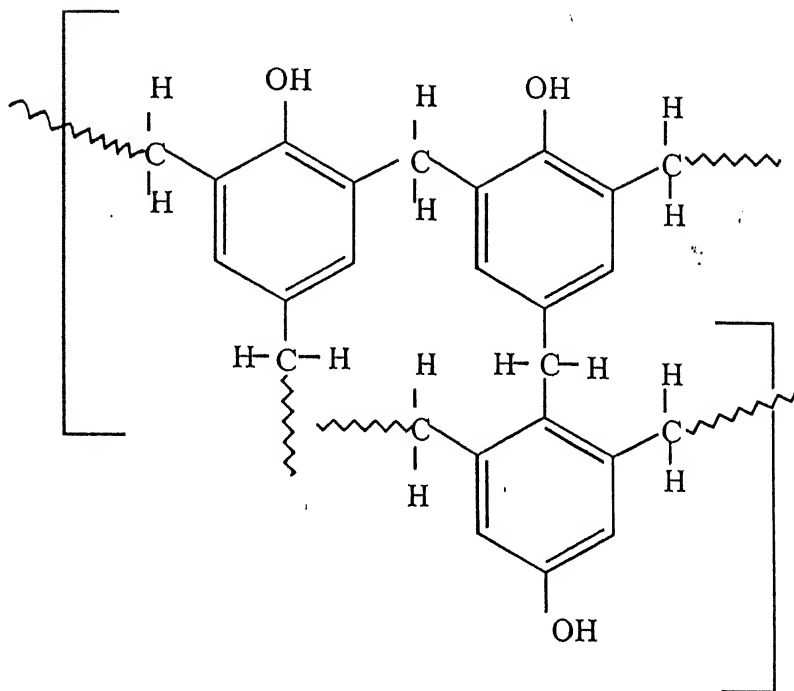
However, complete elimination of the defects appears to be difficult. The calcined clay supports are finally polished by using a silicon carbide abrasive sheet (No C220). The water flow, in the clay supports thus prepared, occurs under atmospheric pressure.

3.3 The resol formation:

The resol polymer (mol.wt.300-700)⁵⁵ is formed in presence of sodium hydroxide with formaldehyde to phenol ratio 1.5 and this is reaction forming the substituted phenols. As the reaction proceeds, methyl of phenols starts condensing to form methylene bridges to give liquid resols. Liquid resols have, on an average, less than two benzene rings per molecule while a solid resol may have as many as three or four. A typical resol may be indicated by the following structure⁴⁶:



When such products with ether linkages are heated, they lose one mole of formaldehyde between them to form a cross-linked polymer having the following structure:



3.4 Membrane casting:

The polished ceramic support is dipped into xylene for 3 hours in order to expel the air present inside the pores. This support is then kept over polyurethane foam (as shown in Figure 2.1), which is soaked in water. This is done to ensure that the polymer doesn't penetrate into the pores of the support and is confirmed by the SEM photograph of the membrane's cross section. The support is coated with resol using a fine knife and allowed to stand at the room temperature for one hour over the wet polyurethane foam. In this period, the top layer becomes dry and the composite support is placed in an oven to cure for 2 hours at 60°C, followed by 12 hours at 120°C. The difference in the weight of the support with and without the polymer is observed. With the knowledge of gain in weight of support upon depositing a thin polymer layer (0.4001g), density of the polymer (2.9 g/cc) and the area of spreading (34.212 cm²), one can easily calculate the thickness of the resol film and it is found as 40.3µm. Upon carbonization of the polymeric film the thickness is reduced to less than 20 µm due to the weight loss during the carbonization process and it is in well consistent with the SEM photographs of cross section of the unmodified carbon-clay composite membranes. Our technique has an advantage that the membrane is cross-linked and sticks well to the clay support, thereby reducing further processing steps.

3.5 The gas phase nitration of carbon-clay composite membranes:

The detailed experimental procedure of gas phase nitration is described in the section 2.4. In the crosslinked resol all the -ortho and -para positions are occupied and after carbonization the remaining hydrogen must be largely due to the methylene linkages. After nitration the points of nitration must have mostly would be the methylene linkages. It may be observed the aliphatic hydrocarbons can not be nitrated by HNO₃, less than temperature of 400°C. However, on nitrating it, with NO_x the reaction occurs readily and about 2000ml of gas reacts easily give the nitrated carbon membrane. The presence of nitro group is confirmed by FT-IR and Raman spectroscopy.

3.6 Amination of the nitrated carbon-clay composite membrane:

To reduce the $-\text{NO}_2$ group to $-\text{NH}_2$ group, we have refluxed the nitrated membrane with LR grade hydrazine hydrate at 75°C for 12 hours. The detailed experimental procedure has been described in section 2.5. By the amination, we found an increase in hydrophilicity of the membrane.

3.7 Elemental analysis (CHN-analysis):

The ultimate elemental analysis of the cured resol is obtained on dry and ash-free basis at different heat treatment temperatures of 120, 200, 300, 400, 500 and 600°C . The CHN analysis is shown in Table 3.1. From this table it is clear that, as the temperature is increased the carbon content is increased and the oxygen content (assuming the rest being is oxygen) is decreased till 500°C . Further, after 500°C , it is found that the carbon content is decreased whereas, that of oxygen is increased at 600°C . The O/C ratio (oxygen content) decreases gradually till 500°C and the started increasing at temperatures greater than 600°C . This is expected because of the carbon-oxygen surface complexes (i.e., C-O, C=O type) desorption from the carbon surface at elevated temperatures⁴⁷.

3.8 Thermogravimetric analysis:

Figure 3.2 shows the thermogravimetric analysis (TGA) of cured resin over the temperature range of 50°C to 800°C at the heating rate of $10^\circ\text{C}/\text{min}$ in N_2 atmosphere. This figure is comparable with that obtained from commercial resol type phenol-formaldehyde beads (PFB) by Kim et al⁴⁸. From this figure it is clear that the thermal degradation is slow upto 350°C . The pyrolysis rate increased from 400°C to 600°C , thereafter the rate slowed down. The overall profile of weight loss by thermal degradation of resol can be divided into five stages. The first stage, upto 200°C is due to loss of moisture and the second stage upto 400°C may be attributed to the loss of some volatiles such as unreacted phenol and formaldehyde, etc. The main degradation of resol occurs at the third stage, just above 400°C , to release the main quantity of gaseous degradation products, such as water, carbon monoxide, carbon dioxide, methane, phenol, cresols and glycols⁴⁹. In the fourth stage (600°C to 800°C), further weight loss can be observed due

carbondioxide, methane, phenol, cresols and xylenols⁴⁹. In the fourth stage (600⁰C to 800⁰C), further weight loss can be observed due to the evolution of some gaseous products such as carbondioxide, methane, benzene, toluene, phenol, cresol and xylenols⁴⁹. Above 800⁰C, it is expected that weight loss may be much higher due to severe gasification of carbon to carbondioxide.

3.9 FT-IR analysis:

The FT-IR spectroscopy was employed to analyze the functional groups present in the liquid resol, unmodified and modified carbon membranes. Figure 3.3 shows the FT-IR spectrum of the resol is identical to that reported by Lin et al⁵⁰. The functional groups corresponding to the major peaks of the spectrum have been identified from reference 51:

- (a) The O-H stretching vibration at 3479.89cm⁻¹ has been observed due to the presence of 2-ethyl phenol.
- (b) The presence of aromatic C-H stretching vibration at 2977.21cm⁻¹ is observed.
- (c) The aliphatic C-H stretching vibrations at 2901.62cm⁻¹ may be because of >CHR or >CH₂ bonding.
- (d) The C-C aromatic ring stretching at 1642.24cm⁻¹ for the presence of aromatic rings.
- (e) The C=O stretching peak at 1261.04cm⁻¹ due to the presence of carbonyl groups.

Similarly the functional groups of unmodified, nitrated and aminated carbon membranes are identified by FT-IR spectrum. Figure 3.4 shows the FT-IR spectra of the unmodified, nitrated and aminated carbon membranes. In case of unmodified carbon membrane an aliphatic C-H stretching is observed at 1441.92cm⁻¹. Likewise, in case of nitrated membrane, its FT-IR clearly shows -NO₂ asymmetric configuration {weak -C(NO₂)₃} at 1592.53 cm⁻¹, -NO₂ symmetric stretching {strong -CH₂-NO₂} is observed at 1381.84cm⁻¹. A weak-medium type R-CHR-NO₂ stretching is observed at 834.67 cm⁻¹, this way confirming the presence of chemically bound nitro groups on the carbon membrane surface. Upon amination, no extra peaks for amine group has been observed but the nitro group peak is disappeared.

3.10 Scanning electron microscope (SEM):

The structural morphology of the surface and cross section have been studied by SEM. Fig 3.4 shows a photograph of the surface of the clay support at 5000 magnifications. In this figure, the photograph suggests that the support is highly porous. In fact, on putting a drop of water on the upper surface, it flows on its own to the other side due to gravity. The white regions in this figure are considered to be clay particles and the spacing between the clay particles are considered to be probable pores.

Figure 3.5 shows the photograph of the top surface of the unmodified carbon-composite membrane at 5000 magnification. The lines which shown up in this figure are due to the scratches while coating the support using a knife and for this reason the latter requires smooth coating. Figure 3.6 show the photographs of the surface of the nitrated carbon membranes in which nitration has occurred for 32 hours at 200°C. In this photograph we observe that there is a change in surface roughness (scratches due to knife coating disappeared) due to the chemical modification done by the nitration reaction. Figure 3.7 show the cross sectional morphology of the unmodified PMMA membranes. This figure clearly shows that the polymer has not penetrated into the pores. We can clearly see the two distinct layers of the polymer and support. This is due to the dipping of the support in water and then casting the membrane on to the wet support. The thickness of the polymer layer in figure is less than 20 μm which is about the same as the thickness calculated from the amount of polymer spread over the support (Table 2.1).

3.11 Raman spectroscopy:

This technique is employed to measure the degree of sp^2 to sp^3 binding in the membrane. Figure 3.8 shows the Raman spectra of the unmodified, nitrated and aminated carbon membranes. The normal spectrum of carbon usually consists of a strong peak in the range of $1580\text{-}1600\text{cm}^{-1}$ and a weak peak in the range of $1350\text{-}1370\text{cm}^{-1}$. The former peak called G-mode peak (G stands for graphite), which represents the graphite structure having sp^2 hybridation and the latter is D-mode peak (D-stands for disorder) having sp^3

hybridation⁵². Graphite is one crystalline form of carbon, in which the atoms are covalently bonded in planar hexagonal arrays with weak secondary bonds between the planes⁵³. From Figure 3.8, we see the presence of G-mode peak at 1591cm^{-1} and the D-mode peak at 1367cm^{-1} . The ratio between their intensities (I_D/I_G) is given in Table 3.2. This ratio increases from 0.85 to 0.95 because of the nitration and amination reactions, even though the individual peak height decrease to the extent that D-mode peaks disappears for the aminated membranes. Since $-\text{C}-\text{NO}_2$ bond normally shows up at 1591cm^{-1} and it is likely that the Raman spectra for the nitrated carbon is showing $-\text{C}-\text{NO}_2$ bond⁵⁴ and its height still decreased for the aminated membranes.

3.12 Small angle X-ray diffraction (XRD):

Figure 3.9 shows the X-ray diffraction patterns of the unmodified nitrated and aminated carbon membranes. In all these three patterns, one can see a broad peak at around a 2θ value of $25-26^\circ$ and a low intensity peak at 2θ value of 50° . These peaks having "h k l" values of the planes are $[0\ 0\ 2]$ and $[1\ 0]$ respectively, which represents the presence of graphite structure. The d_{002} value is traditionally used to estimate a graphitization degree of the carbon. In general, growing disorder in the materials can be represented by increase in value of d_{002} . By the nitration and amination of the carbon membrane, it is becoming increasingly amorphous in nature.

3.13 Determination of molecular weight cut-off (MWCO) of the membranes:

The MWCO is given by the smallest molecular mass of the macrosolute, which is 90% retained by the membrane. Very dilute solutions (1 wt.%) of macrosolutes are used for determining the MWCO. The macrosolutes are preferably rigid and globular molecules and has to be monodispersed and should be soluble in water. In this work we have used polyethylene glycol (PEG) of different molecular weights ranging from 200 to 35000. To calibrate the refractometer we have prepared different PEG solutions of varying concentrations. The calibration data have been shown in Fig 3.10 (and Table 3.3). For each run the ultrafiltration cell is filled with 500 ml of the feed. All the membranes have been flushed with distilled water at 100 psig to remove the strongly

adsorbed gases inside the pores. For determining MWCO, we have fixed the pressure at 60 psig throughout these experiments. The permeate and retentate have been collected after 24 hours and their concentrations are measured using the refractometer.

The experimental results for MWCO of the unmodified and nitrated membranes are shown in Table 3.4 and 3.5 respectively and the cut-off curves are shown in Fig 3.11. From this figure we have obtained the MWCO of the membranes corresponding to 90% rejection of PEG solutions used. The MWCO of the unmodified carbon membrane is observed to be 7500 and that of the nitrated membrane has an MWCO of 14000. This data is in good agreement with the SEM observation (Fig 3.5 and Fig 3.6) that there is an increase in pore size due to the nitration reaction.

3.14 Separation experiments using aqueous solution of chromic acid solution:

We have carried out the separation experiment with 1000ppm concentration of chromic acid solution. The concentration of the solution has been measured by using conductivity cell (Century CMK, μ p based water analysis kit) with 0.1 μ mho accuracy. The instrument is calibrated with different concentration of chromic acid solution. The calibration data is shown in Table 3.6 and in Figure 3.12. For each run the ultrafiltration cell is filled with 500ml of chromic acid solution and the permeate flux is measured after 24 hours for each pressure. The results obtained with the unmodified, nitrated and aminated membranes have been listed in Table 3.7, 3.8 and 3.9 respectively. The pure water flux curves, solute flux curves and rejection curves are shown in Figure 3.13, 3.14 and 3.15 for the unmodified, nitrated and aminated membranes respectively. From Figure 3.13 it is clear that the pure water flux is linearly increased with increase in pressure. This figure also reveals that by the nitration reactions, the pure water flux is increased more than two times. The water flux of the aminated membrane is still higher than that of the unmodified membrane, whereas the difference in flux is low between the nitrated and aminated membranes. From this we can infer that by the amination reaction the hydrophilicity of the membrane is increased.

Figure 3.14 shows that the solute flux is linearly increased with increase in pressure for the case of the unmodified, nitrated and aminated membranes. By the

nitration and amination modifications, the slope of these curves are much higher (3times). The difference in flux however is low between the nitrated and aminated membranes and the increase could be attributed to the hydrophilicity of the membrane due to the modification reactions. From Figure 3.15, the rejection would reach a plateau with pressures and thereafter start decreasing. However for the pressure range studied we did not find this phenomena.

Table 3.1 Elemental analysis of resol at different heat treatment temperatures:

S.No.	Temperature (°C)	%C	%H	%N	%O	O/C
1	120	49.7350	4.4020	0.0000	45.8630	0.9221
2	200	71.9376	6.4728	0.1020	21.4876	0.2987
3	300	72.2495	7.2412	0.1325	20.8768	0.2890
4	400	74.2478	6.9090	0.1353	18.7079	0.2520
5	500	76.7965	4.4295	0.0000	18.7740	0.2445
6	600	70.3963	2.8853	0.1765	26.5419	0.3770

Table 3.2 The R values for the unmodified, nitrated and aminated membraes:

Membrane	I _D	I _G	R = I _D /I _G
Unmodified	2900	3400	0.8529
Nitrated	2600	3000	0.8667
Aminated	1800	1900	0.9474

Table 3.3 Calibration data for different molecular weight of PEG solutions:

Concentration of PEG (wt.%)	Refractive index
10.000	1.3430
5.000	1.3370
2.500	1.3340
1.250	1.3325
0.625	1.3315
0.000	1.3310

Table 3.4 Molecular weight cut-off of the unmodified carbon-clay composite membrane:

Molecular weight of PEG	Permeate		Retentate		% Rejection
	Refractive index of permeate	Concentration of permeate (wt. %)	Refractive index of retentate	Concentration of retentate (wt. %)	
400	1.3320	1.000	1.3320	1.00	0.00
600	1.3318	0.850	1.3320	1.00	15.00
4000	1.3314	0.575	1.3320	1.00	42.50
6000	1.3311	0.275	1.3320	1.00	72.50
12000	1.3310	0.000	1.3320	1.00	100.00
20000	1.3310	0.000	1.3320	1.00	100.00
35000	1.3310	0.000	1.3320	1.00	100.00

Table 3.5 Molecular weight cut-off of the nitrated carbon-clay composite membrane:

Molecular weight of PEG	Permeate		Retentate		% Rejection
	Refractive index of permeate	Concentration of permeate (wt. %)	Refractive index of retentate	Concentration of retentate (wt. %)	
400	1.3320	1.000	1.3320	1.00	0.00
600	1.3320	1.000	1.3320	1.00	0.00
4000	1.3316	0.675	1.3320	1.00	32.50
6000	1.3314	0.550	1.3320	1.00	45.00
12000	1.3312	0.300	1.3320	1.00	70.00
20000	1.3310	0.000	1.3320	1.00	100.00
35000	1.3310	0.000	1.3320	1.00	100.00

Table 3.6 Calibration data for chromic acid solution of different concentrations:

Concentration of chromic acid (mg/lit)	Conductivity (mmho)
1000	4.435
500	2.20
250	1.100
125	0.550

Table 3.7 Results of the separation experiments done with unmodified carbon-clay composite membrane with 1000 mg/lit aqueous chromic acid solution:

Applied pressure (psig)	Pure water flux (l /m ² hr)	Permeate flux(l /m ² hr)	Permeate	
			Conductivity(mmho)	Concentration(mg/lit)
20	1.0128	0.4655	2.09	475.000
30	1.3376	0.6767	1.91	434.091
40	1.6101	0.8538	1.89	429.545
50	2.2664	1.0809	1.76	400.000
60	2.2914	1.1218	1.60	363.636
70	2.5525	1.1854	1.30	295.455

Applied pressure (psig)	Retentate		% Rejection $\left(1 - \frac{C_P^{sol}}{C_R^{sol}}\right) \times 100$
	Conductivity (mmho)	Concentration (mg/lit)	
20	4.4	1000	52.500
30	4.4	1000	56.591
40	4.4	1000	57.045
50	4.4	1000	60.000
60	4.4	1000	63.636
70	4.4	1000	70.455

Table 3.8 Results of the separation experiments done with nitrated carbon-clay composite membrane with 1000 mg/lit aqueous chromic acid solution:

Applied pressure (psig)	Pure water flux (l /m ² hr)	Permeate flux(l /m ² hr)	Permeate	
			Conductivity(mmho)	Concentration(mg/iit)
20	1.8599	1.0242	2.68	609.091
30	2.1528	1.4171	2.43	552.273
40	2.4798	1.6146	2.27	515.909
50	3.1634	2.4912	2.16	490.909
60	3.4337	2.7955	2.00	454.545
70	3.8628	3.2769	1.88	427.273

Applied pressure (psig)	Retentate		% Rejection $\left(1 - \frac{C_P^{sol}}{C_R^{sol}}\right) \times 100$
	Conductivity (mmho)	Concentration (mg/lit)	
20	4.4	1000	39.091
30	4.4	1000	44.773
40	4.4	1000	48.409
50	4.4	1000	50.909
60	4.4	1000	54.545
70	4.4	1000	57.273

Table 3.9 Results of the separation experiments done with aminated carbon-clay composite membrane with 1000 mg/lit aqueous chromic acid solution:

Applied pressure (psig)	Pure water flux (l /m ² hr)	Permeate flux(l /m ² hr)	Permeate	
			Conductivity(mmho)	Concentration(mg/lit)
20	2.1665	1.2581	2.68	609.091
30	2.2959	1.6033	2.44	554.545
40	2.7592	2.1778	2.28	518.909
50	3.4132	2.5230	2.16	490.909
60	3.9469	2.9885	1.98	450.000
70	4.5532	3.4882	1.85	420.454

Applied pressure (psig)	Retentate		% Rejection $\left(1 - \frac{C_P^{sol}}{C_R^{sol}}\right) \times 100$
	Conductivity (mmho)	Concentration (mg/lit)	
20	4.4	1000	39.091
30	4.4	1000	44.545
40	4.4	1000	48.109
50	4.4	1000	50.909
60	4.4	1000	55.000
70	4.4	1000	57.955

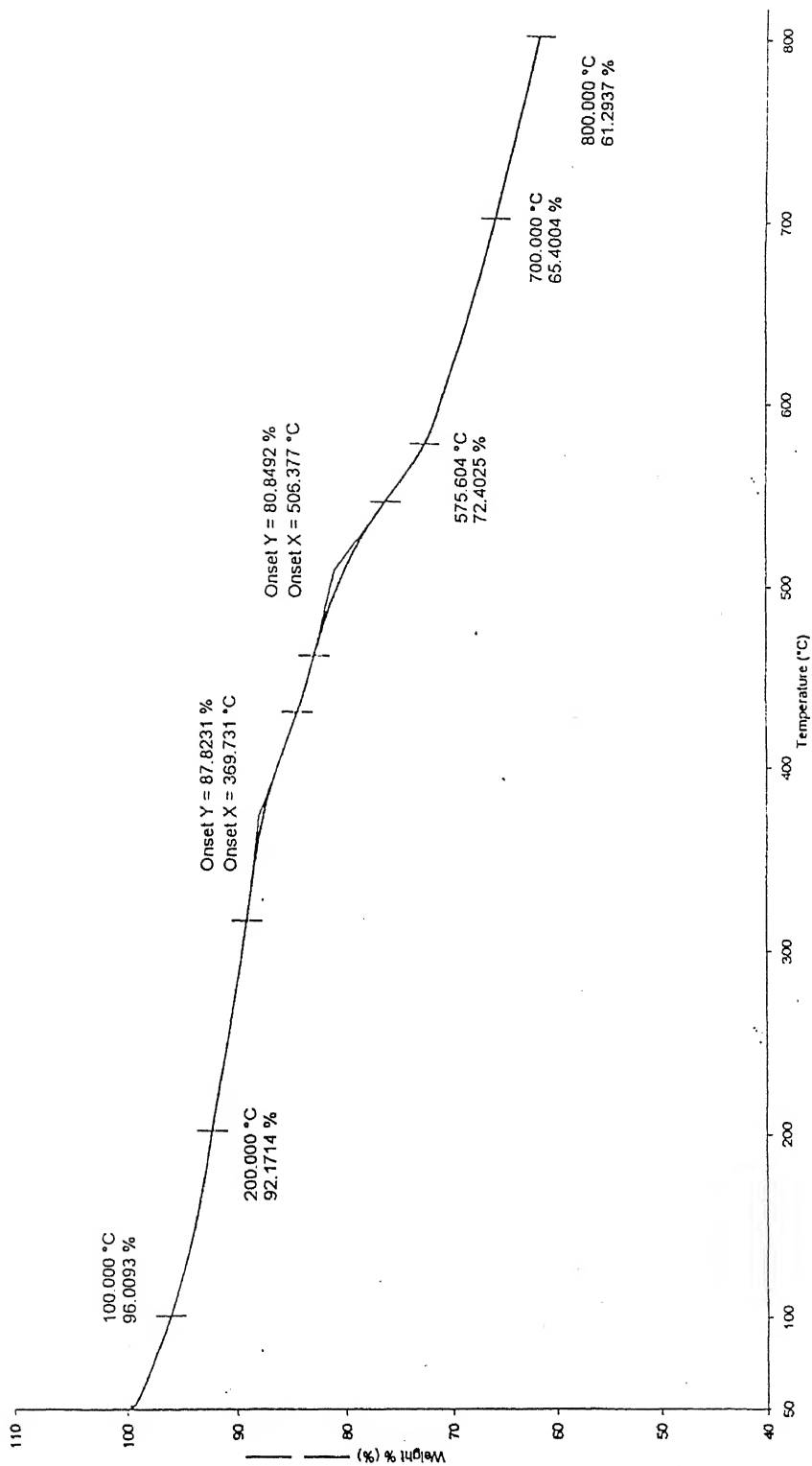


Figure 3.1 Thermogravimetric analysis of the cured resol under N_2 atmosphere

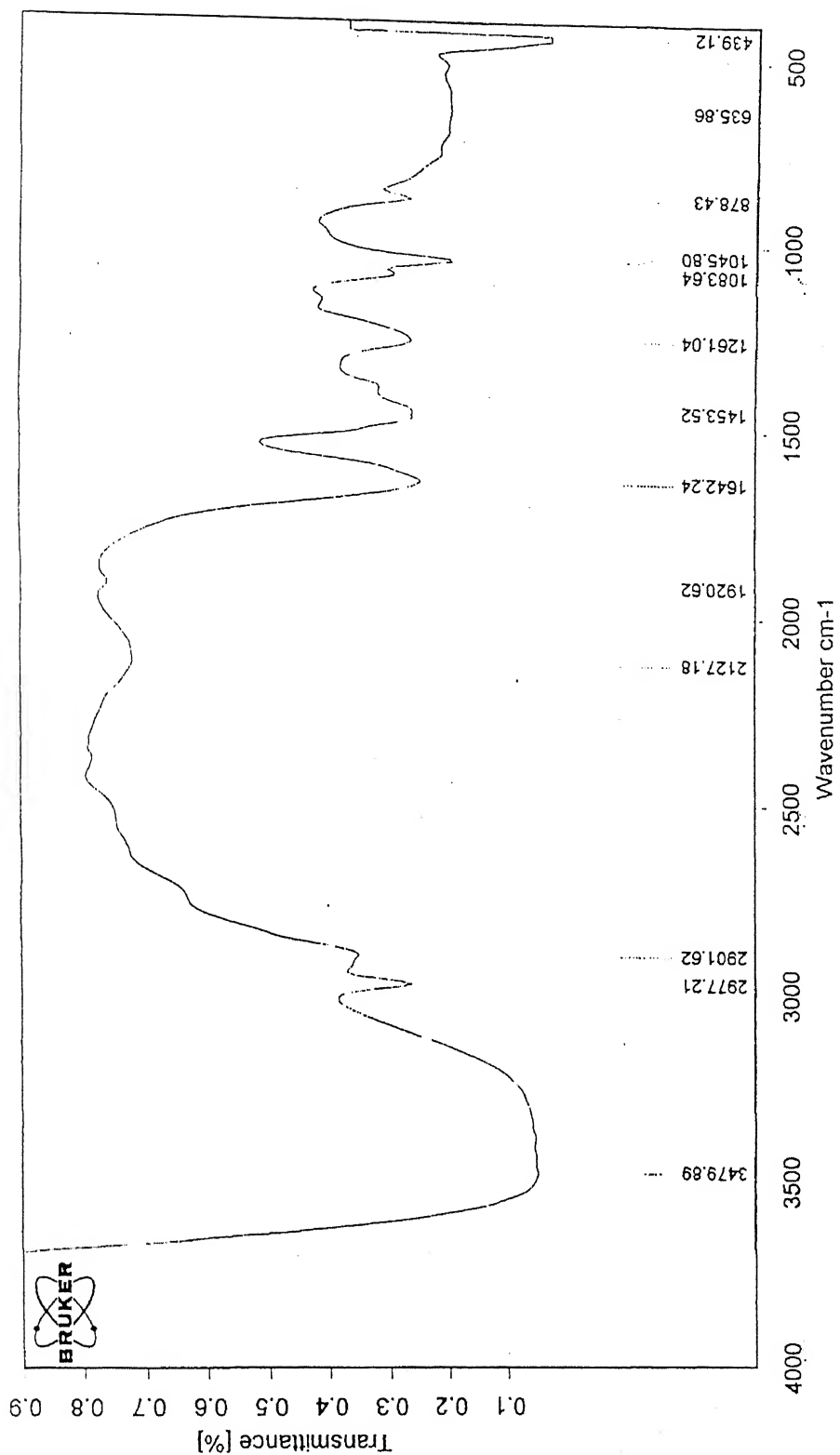


Figure 3.2 The FT-IR spectrum of the resol type PF resin catalyzed by NaOH

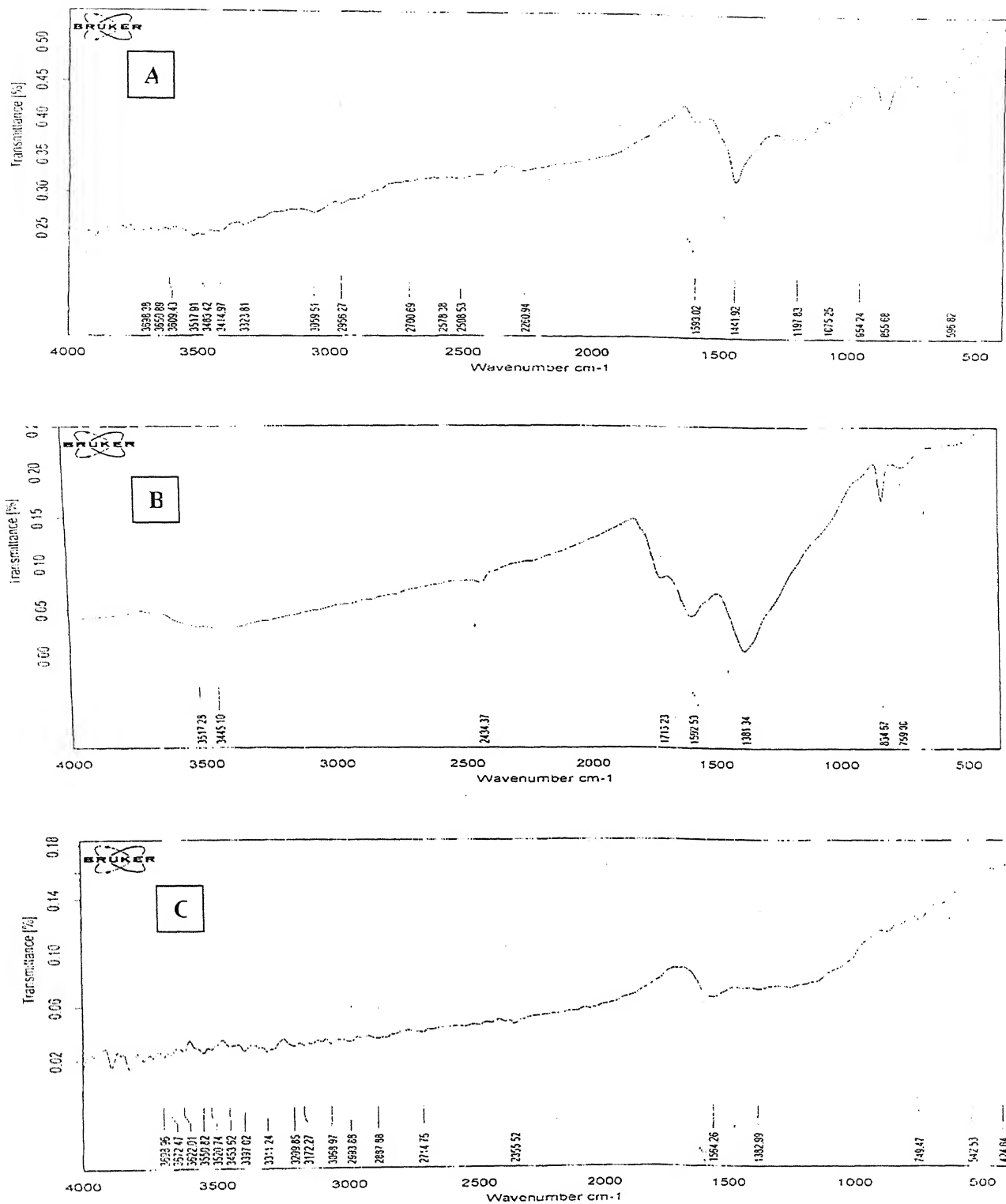


Figure 3.3 The FT-IR spectra of (A) Unmodified, (B) Nitrated and (C) Aminated carbon membranes

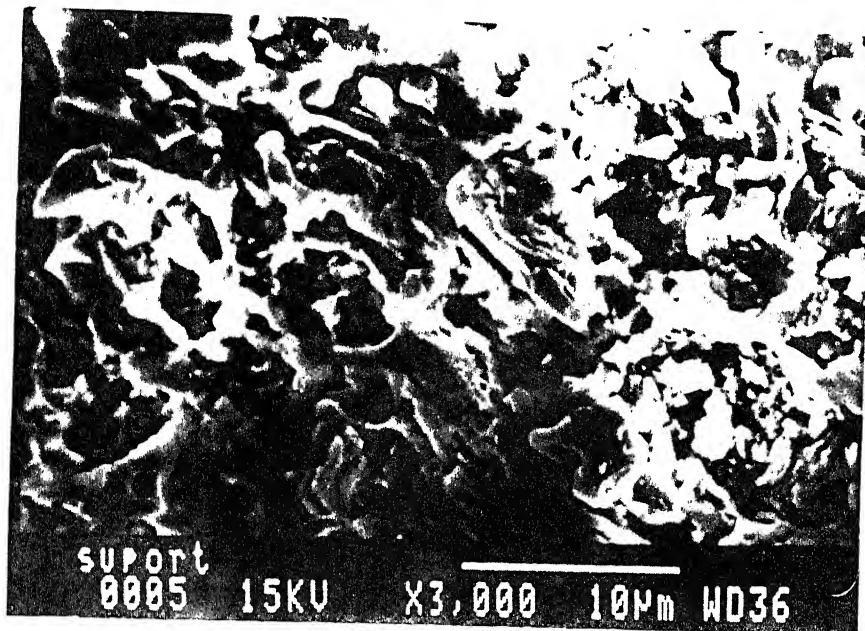


Figure 3.4 The SEM photograph of the top surface of the clay support

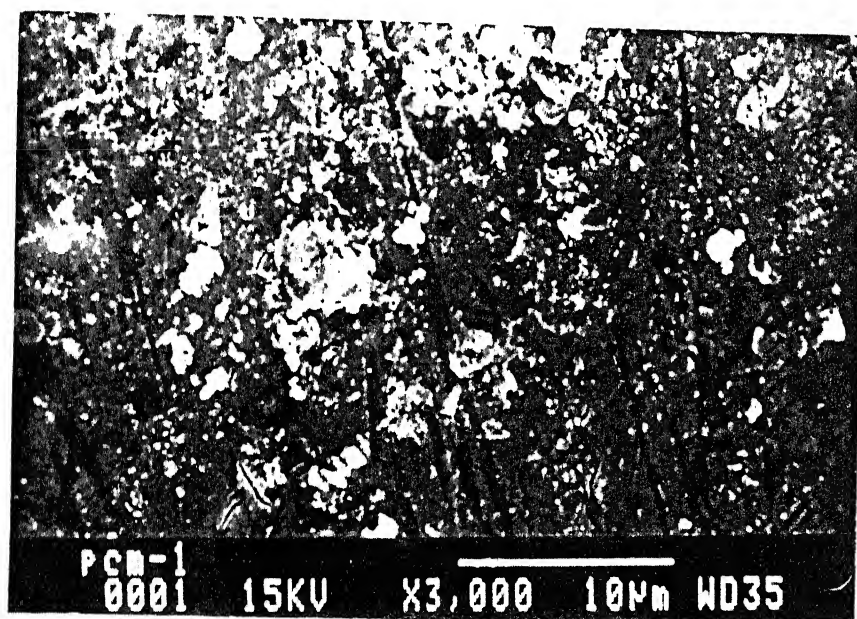


Figure 3.5 The SEM photograph of the top surface of the unmodified carbon membrane

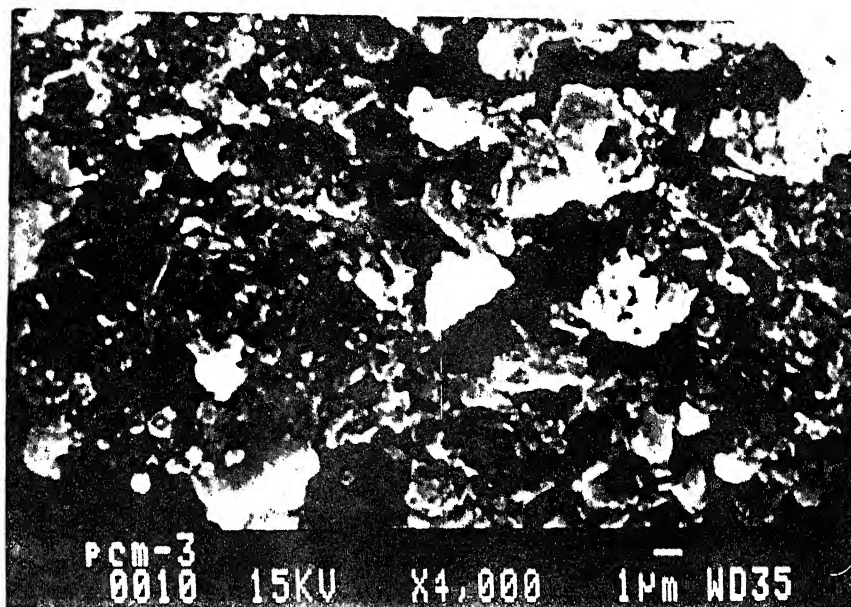


Figure 3.6 The SEM photograph of the top surface of the nitrated carbon membrane



Figure 3.7 The SEM photograph of the top surface of the cross-section of the carbon membrane

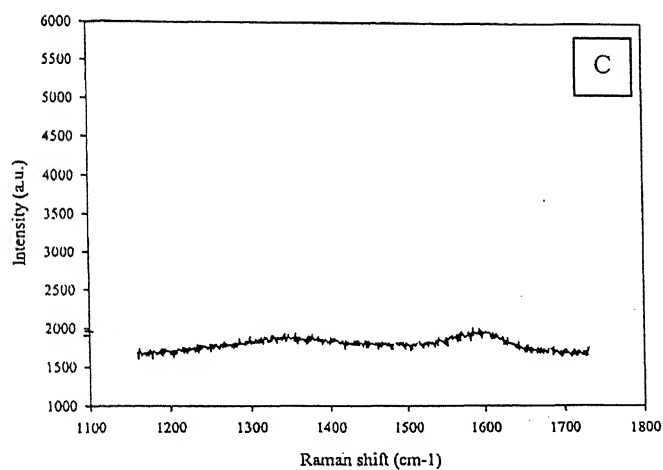
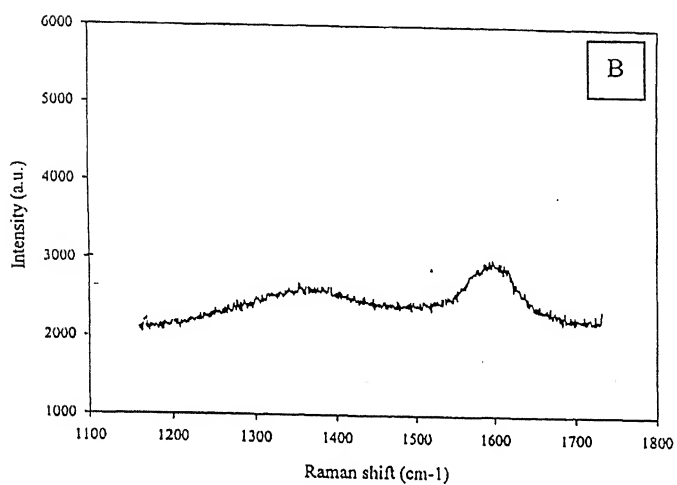
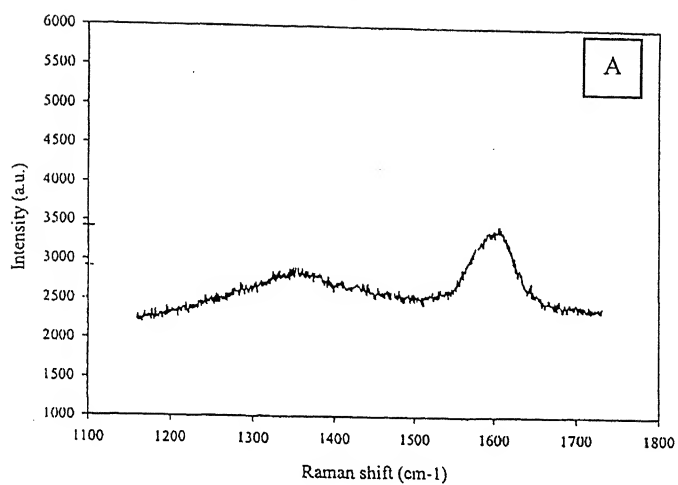


Figure 3.8 The Raman spectra of (A) Unmodified, (B) Nitrated and (C) Aminated carbon membranes

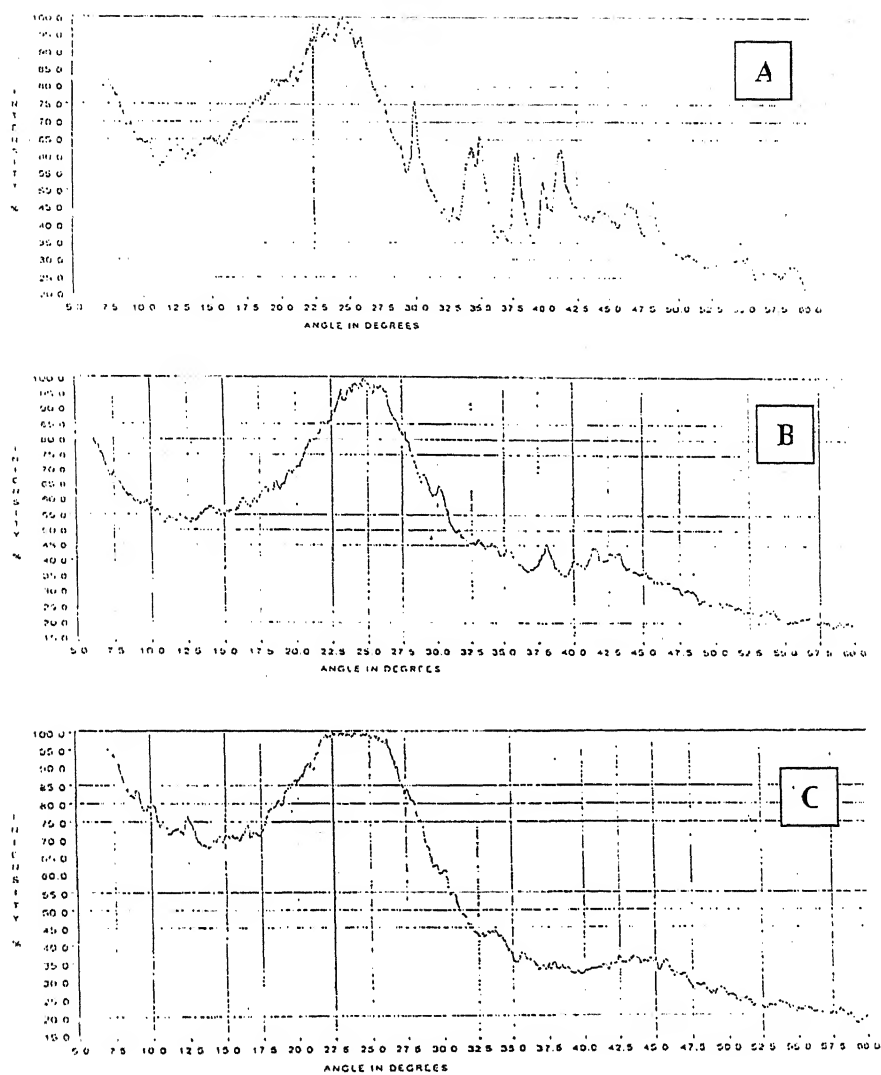


Figure 3.9 The XRD patterns of the (A) Unmodified, (B) Nitrated and (C) Aminated carbon membranes

Calibration curve for Polyethylene Glycol

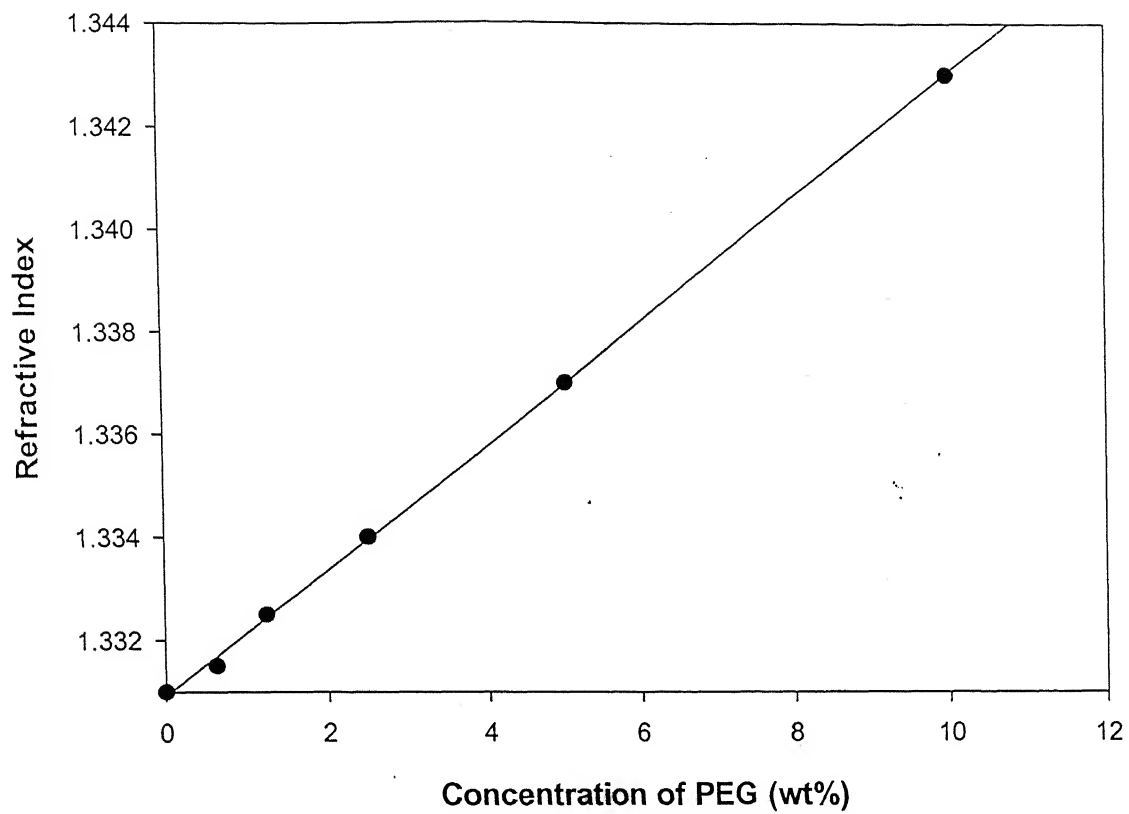


Figure 3.10 The calibration curve for the Polyethylene Glycol

Molecular weight cut-off curves

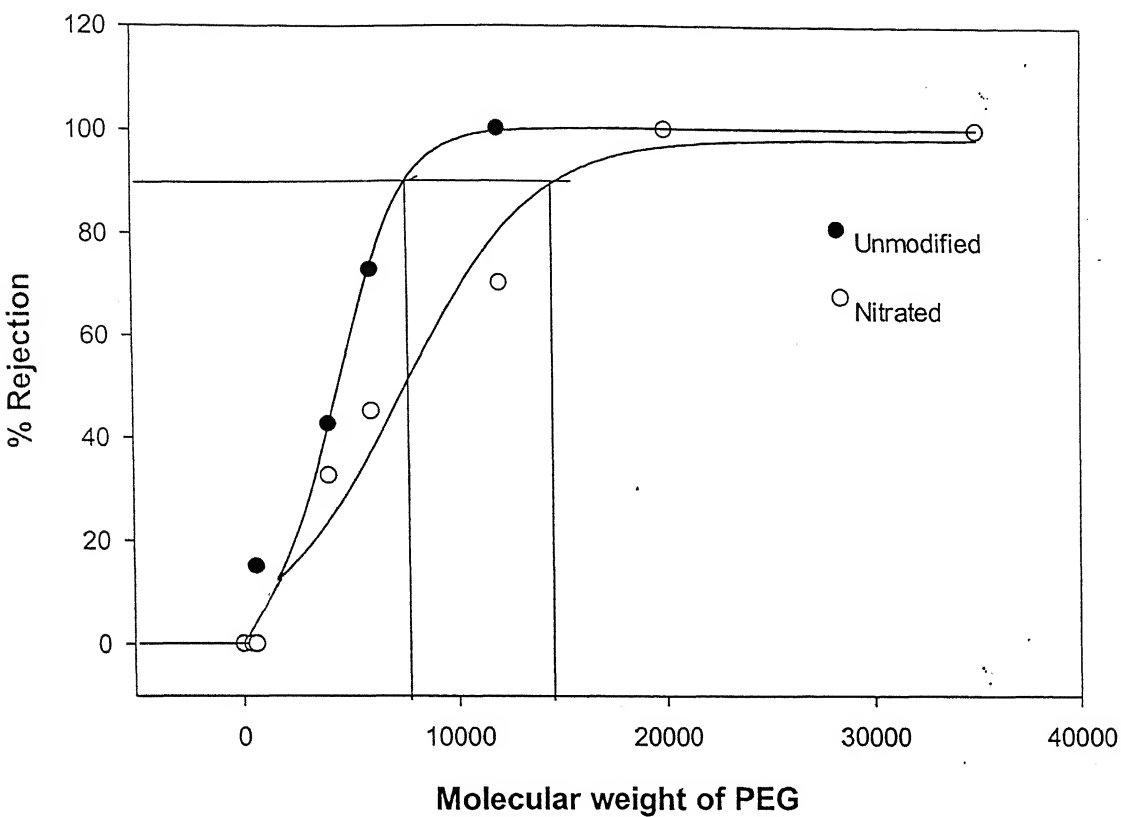


Figure 3.11 The molecular weight cut-off curves for the unmodified and nitrated carbon membrane

Concentration (mg/l)	Conductivity (mmho)
120	0.55
250	1.1
500	2.2
1000	4.4

51

water flux curves

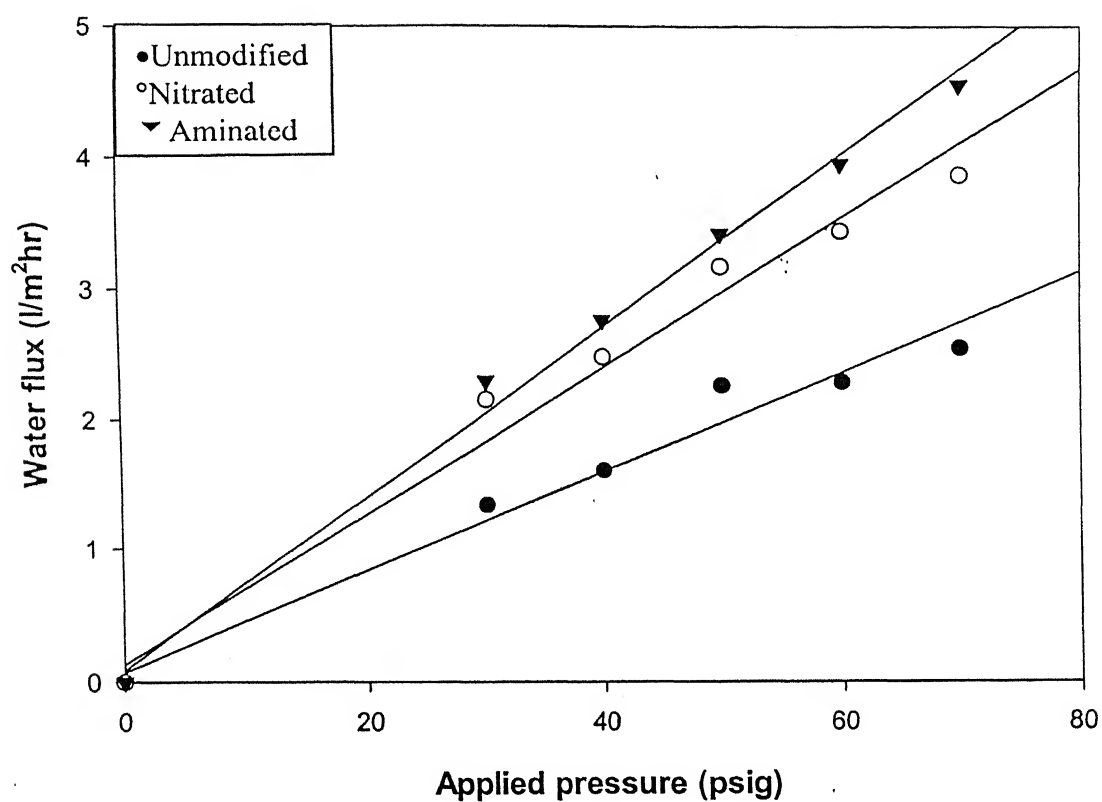


Figure 3.13 The water flux curves for the unmodified, nitrated and aminated carbon membrane

Solute flux curves

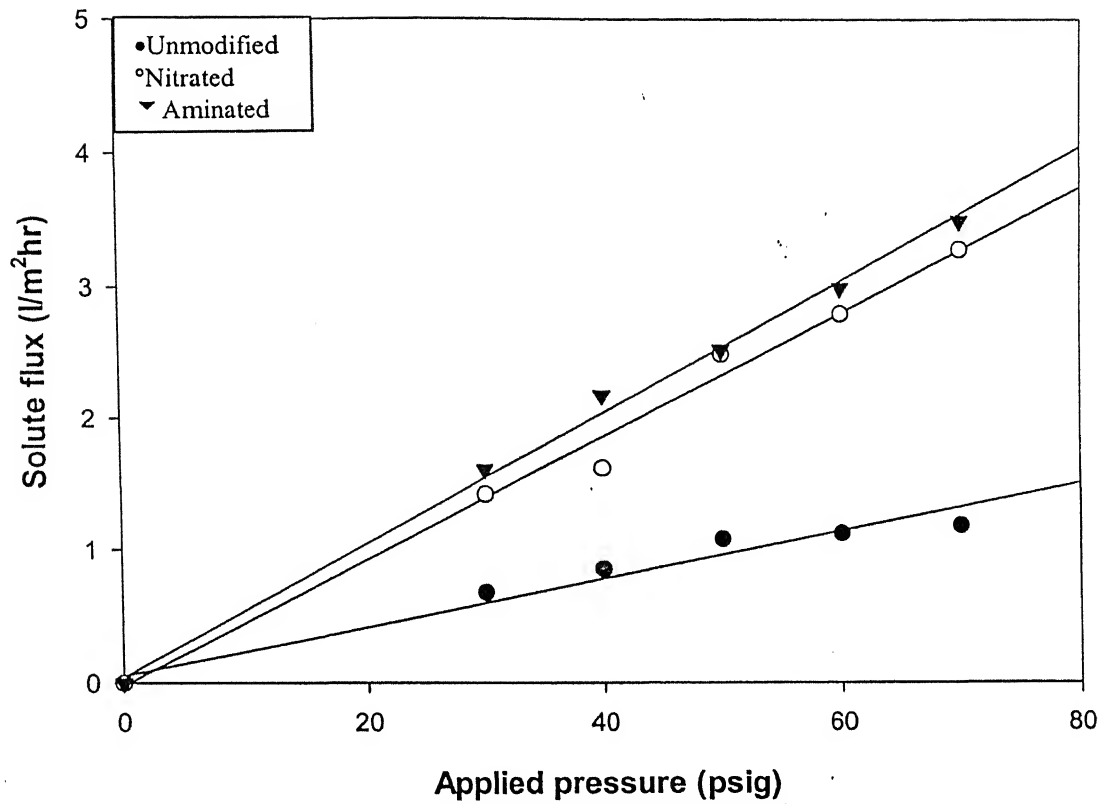


Figure 3.14 The solute flux curves for the unmodified, nitrated and aminated carbon membranes

Rejection curves

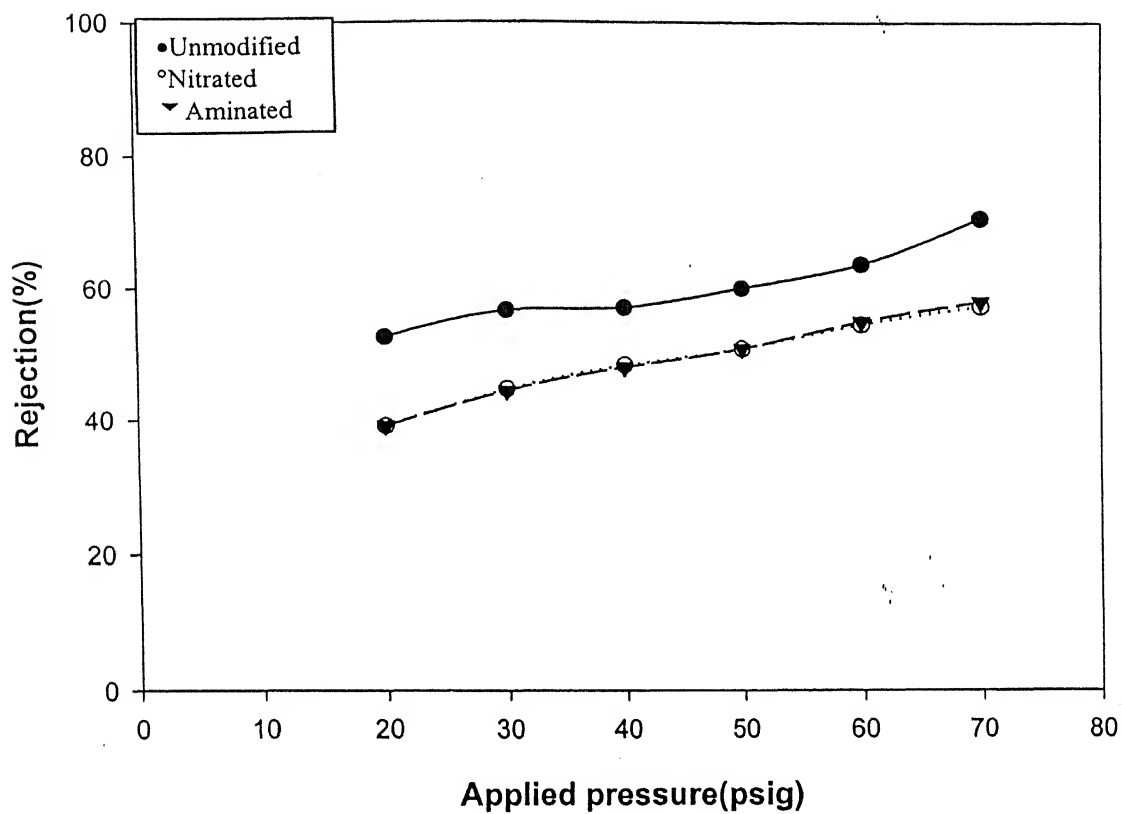


Figure 3.15 The rejection curves for the unmodified, nitrated and aminated carbon membranes

Chapter-4

Conclusions

1. The resol polymer (300-700 mol.wt.) was found to be a suitable precursor material for the preparation of the porous carbon-clay composite membranes, as it would stick nicely to the clay support.
2. The membrane has been prepared by the knife coating technique followed by carbonization in a closed chamber at 500⁰C for half an hour.
3. The carbon membrane has been modified by the gas phase nitration reaction and the presences of the nitro groups have been confirmed by the FT-IR anlaysis.
4. These nitro groups have been further reduced to amine groups, by treating with hydrazine hydrate. The FT-IR of the aminated membrane shows the absence of the nitro peak at 1381cm⁻¹.
5. From the XRD and Raman spectra, it is found that prepared carbon membrane is partially graphitized. Upon, the nitration, the D-peak intensity in Raman spectra is found to decrease and by the amination it disappears completely. As opposed to this, in the XRD patterns of the modified membrane, the [1 0] peak disappears and confirms that the material has become amorphous in nature.
6. The calculated MWCO for the unmodified and nitrated membranes were determined to be 7500 and 14000 respectively.
7. Separation experiments have been carried out using 1000ppm aqueous chromic acid solution and the rejection is found increase with increase in pressure. The pure water and solute flux is increased more than two times for modified membrane compared to those for unmodified membrane and can be attributed to the increased hydrophilicity by the modification reactions.

References: -

1. K. Scott, R. Hughes, Industrial membrane separation technology, Blackie Academic & Professional, 1996.
2. H.P.Hsich, Inorganic Membranes, Membr. Mater. Proc., **84**(1990) 1.
3. A.F. Ismail, L.I.B. David, A review on the latest development of carbon membranes for gas separation, J. Membr. Sci., **193**(2001) 1- 18.
4. J.E. Koresch, A. Soffer, The carbon molecular sieve membranes, General properties and the permeability of CH₄/H₂ mixture, Sep. Sci. Technol., **22**(1987) 973.
5. M.B. Rao, S. Sircar, Nanoporous carbon membrane for gas separation, Gas Sep. Purif., **7**(1993) 279.
6. C.H. Liang, G.Y. Sha, S.C. Guo, Carbon membrane for gas separation derived from coaltar pitch, Carbon, **37**(1999) 1391.
7. J. Peterson, M. Matsuda, K. Haraya, Capillary carbon molecular sieve membranes derived from kapton for high temperature gas separation, J. Membr. Sci., **131**(1997) 85.
8. A.B. Fuertes, T.A. Centeno, Preparation of supported asymmetric carbon molecular sieve membranes, J. Membr. Sci., **144**(1998) 105-111.
9. T.A. Centeno, A.B. Fuertes, Supported carbon molecular sieve membranes based on a phenolic resin, J. Membr. Sci., **160**(1999) 201-211.
10. T.A. Centeno, A.B. Fuertes, Carbon molecular sieve membranes derived from a phenolic resin supported on porous ceramic tube, sep. sci. technol., **25**(2001) 379-384.
11. M. Acharya, H.C. Foley, Spray-coating of nanoporous carbon membranes for air separation, J. Membr. Sci., **161**(1999) 1-5.
12. M.S. Strano, H.C. Foley, Synthesis and Characterization of Catalytic Nanoporous Carbon Membranes, AIChE J., **47**(1)(2001) 66-78.
13. F.K. Katsaros, T.A. Steriotis, A.K. Subos, A. Mitropoulos, N.K. Kanellopoulos, S. Tennison, High pressure gas permeability of microporous carbon membranes, micropor. Mater., **8**(1997) 171-176.

14. L.E. Sojo, A. Brocke, J. Fillion, S.M. Price, Application of activated carbon membranes for on-line cleanup of vegetable and fruit extracts in the determination of pesticide multiresidues by gas chromatography with mass selective detection, *J. Chromatogr. A*, **788**(1997) 141-154.
15. I. Menendez, A.B. Fuertes, Aging of carbon membranes under different environments, *carbon* **39**(2001) 733-740.
16. M.S. Strano, A.L. Zydney, H. Barth, G. Wooley, H. Agarwal, H.C. Foley, Ultrafiltration membrane synthesis by nanoscale templating of porous carbon, *J. Membr. Sci.*, **198**(2002) 173-186.
17. Y.Y. Li, T. Nomura, A. Sakoda, M. Suzuki, Fabrication of carbon coated ceramic membranes by pyrolysis of methane using a modified chemical vapor deposition apparatus, *J. Membr. Sci.*, **197**(2002) 23-35.
18. D.S. Lafyatis, J. Tung, H.C. Foley, Poly (furfuryl alcohol) – Derived Carbon Molecular Sieves: Dependence of Adsorptive Properties on Carbonization Temperature, Time, and Poly (ethylene glycol) Additives, *Ind. Eng. Chem. Res.*, **30**(1991) 865-873.
19. M.G. Sedigh, M. Jahangiri, P.K.T. Liu, M. Sahimi, T.T. Tsotsis, Structural Characterization of Polyetherimide-based carbon Molecular Sieve Membranes, *AIChE J.*, **46**(11)(2000) 2245-2255.
20. M. Acharya, B.A. Raich, H.C. Foley, M.P. Harold, J.J. Lerou, Metal-Supported Carbogenic Molecular Sieve Membranes: Synthesis and Applications, *Ind. Eng. Chem. Res.*, **36**(1997) 2924-2930.
21. W. Wei, H. Hu, L. You, G. Chen, Preparation of carbon molecular sieve membrane from phenol-formaldehyde Novolac resin, *Carbon* **40**(2002) 445-467.
22. C.W. Jones, W.J. Kores, Characterization of Ultramicroporous Carbon Membranes with Humidified Feeds, *Ind. Eng. Chem. Res.*, **34**(1995) 158-163.
23. A.B. Fuertes, Effect of air oxidation on gas separation properties of adsorption-selective carbon membranes, *carbon* **39**(2001) 697-706.
24. Y.D. Chen and R.T. Yang, Preparation of Carbon Molecular Sieve Membrane and Diffusion of Binary Mixtures in the Membrane, *Ind. Eng. Chem. Res.*, **33**(1994) 3146-3153.

25. A.B. Fuertes, Adsorption-selective carbon membranes for gas separation, *J. Membr. Sci.*, **177**(2000) 9-16.
26. W. Shusen, Z. Meiyun, W. Zhizhong, Asymmetric molecular sieve carbon membranes, *J. Membr. Sci.*, **109**(1996) 267-270.
27. V.C. Geiszler, W.J. Koros, Effects of polyimide pyrolysis conditions on carbon molecular sieve membrane properties, *Ind. Eng. Chem. Res.*, **35**(1996) 2999-3003.
28. J. Hyashi, H. Mizuta, M. Yamamoto, K. Kusakabe, S. Morooka, S.H. Suh, *Ind. Eng. Chem. Res.*, **35**(1996) 4176-4181.
29. M.B. Rao, S. Sircar, Nanoporous carbon membranes for separation of gas mixtures by selective surface flow, *J. Membr. Sci.*, **85**(1993) 253-264.
30. R.K. Mariwala, H.C. Foley, Evolution of Ultramicroporous Adsorptive Structure in Poly(furfuryl alcohol)- Derived Carbogenic Molecular Sieves, *Ind. Eng. Chem. Res.*, **33**(1994) 607-615.
31. W. Reinmann, I. Yeo, Ultrafiltration of Agricultural Waste Water with organic and inorganic membranes, *Desalination*, **109**(1997) 263-267.
32. A. Hafiane, D. Lemordant, M. Dhab, Removal of hexavalent chromium by nanofiltration, *Desalination*, **130**(2000) 305-312.
33. A. Cassano, E. Drioli, R. Molinari, Recovery and reuse of chemicals in unhairing, degreasing and chromium tanning processes by membranes, *Desalination*, **113**(1997) 251-161.
34. A.I. Hafez, M.S. El-Manharawy, M.A. Khedr, RO membrane removal of unreacted chromium from spent tanning effluent. A pilot-scale study, part2, *Desalination*, **144** (2002) 237-242.
35. A.K. Chakaravarti, S.B. Chowdhury, S. Chakrabarty, T. Chakarabarty, D.C. Mukherjee, Liquid membrane multiple emulsion process of chromium (VI) separation from waste waters, *Colloids and Surfaces, A: Physicochemical and Engineering Aspects*, **103** (1995) 59-71.
36. P. Gao, X. Gu, T. Zhou, New separation method for chromium (VI) in water by collection of its ternary complex on an organic solvent-soluble membrane filter, *Analytica chimica acta* **332** (1996) 307-312.

37. K. Scott, A.O. Ibadan, An integrated electro- ' Ratio in Resin Synthesis
membrane approach to recycling, *Electrochimic* 'a resins, *Ind. Eng.*
850.
38. R. Chiarizia, Application of supported liquid mem ' and
technetium (VII) and chromium (VI) from ground wat
39-64.
39. J.G. Rao, B.G.S. Prasad, V. Narasimhan, T. Ramasami,
Electrodialysis in the recovery and reuse of chromium from
Membr. Sci., **46** (1989) 215-224.
40. E.L.Cussler, D.F. Evans, Liquid membranes for separations and rea , *J. Membr.*
Sci., **6** (1980) 113-121.
41. E.R. Gues, M.J. den Exter, H.V. Bekkum, Synthesis and characterization of zeolite
(MFI) membranes on porous ceramic support, *J. Chem. Soc. Faraday Trans*, **88**
(1992) 3101-3109.
42. A. Ravve, Principles of polymer chemistry, Plenum press, Newyork, 1995.
43. A. Knop, L.A. Plato, Phenolic Resins-Chemistry, Applications and performance,
Springer Verlag, 1985.
44. W.J. Koros, Y.H. Ma, T. Schimidzu, Terminology for membranes and membrane
processes, *J. Membr. Sci.*, **120** (1996) 149-159.
45. J.S. Reed, Introduction to the principles of ceramic processing, John Wiley & Sons,
Newyork, 1989.
46. R. Sinha, Outlines of polymer technology, Manufacture of polymers, Prentice Hall of
India, Pvt. Ltd., 2000.
47. R. Kostecki, B. Schnyder, D. Alliata, X. Sang, K. Kinoshita, R. Kotz, Surface studies
of carbon films from pyrolyzed photoresist, *Thin Solid Films*, **396** (2001) 36-43.
48. M.H Kim, C.H. Yun, Y.J. Kim, C.R. Park, M. Inagaki, Changes in pore properties of
phenol formaldehyde-based carbon with carbonization and oxidation conditions,
Carbon, **40**(2002) 2003-2012.
49. S.R. Tennison, Phenolic-resin-derived activated carbons, *Appl. Cat. A*, **173**(1998)
289-311.

50. C.C.Lin, H..Teng, Influence of the Formaldehyde-to-Phenol Ratio in Resin Synthesis on the Production of Activated Carbons from Phenol-Formaldehyde resins, Ind. Eng. Chem. Res., **41**(2002) 1986-1992.
51. D.L. Vien, N.B. Colthup, M.G. Fateley, J.G. Grasselli, The handbook of infrared and Raman characteristic frequencies of organic molecules, Academic Press, 1991.
52. C.C.M. Ma, J.M. Lin, W.C. Chang, T.H. Ko, Carbon/carbon nano composites derived from phenolic resin-silica hybrid ceramers: microstructure, physical and morphological properties, Carbon **40** (2002) 977-984.
53. W.G. Moffatt, G.W. Pearsall, J. Wulff, Structure, John Wiley & Sons, Inc., 1964.
54. H. Baraksha, A. Labudzinska, J. Terpinski, Laser Raman spectrometry analytical applications, PWN-Polish Scientific Publishers, 1987.
- W.R. Sorenson, Preparative methods of polymer chemistry, Inter Science Publishers, 1968.